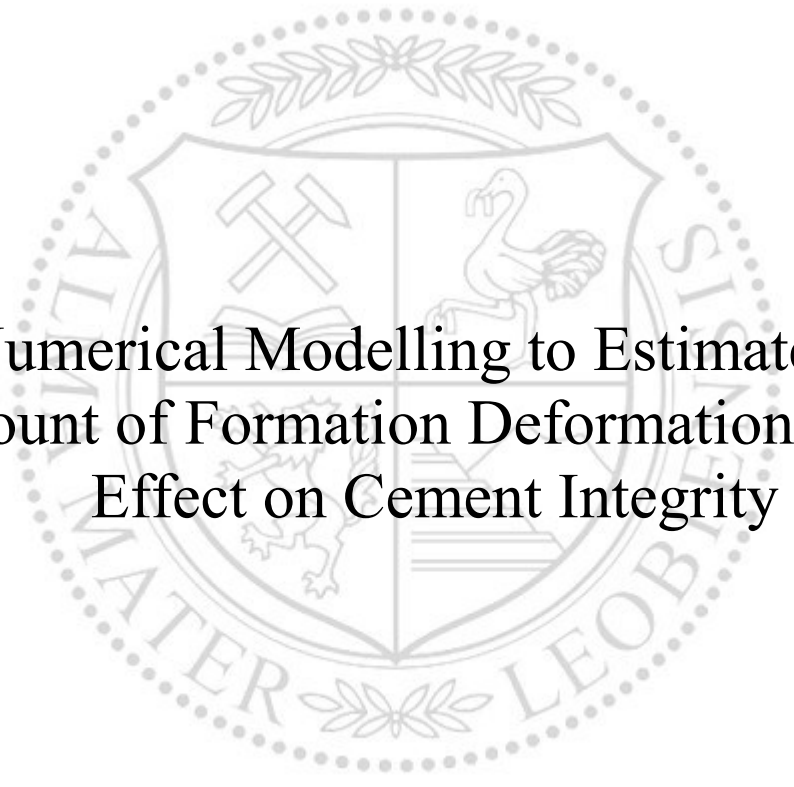Chair of Drilling and Completion Engineering

# Master's Thesis

# Numerical Modelling to Estimate the Amount of Formation Deformation and its Effect on Cement Integrity

## Timothy Atkin

May 2019

## AFFIDAVIT

I declare on oath that I wrote this thesis independently, did not use other than the specified sources and aids, and did not otherwise use any unauthorized aids.

I declare that I have read, understood, and complied with the guidelines of the senate of the Montanuniversität Leoben for "Good Scientific Practice".

Furthermore, I declare that the electronic and printed version of the submitted thesis are identical, both, formally and with regard to content.

Date 21.05.2019

Signature Author
Timothy Atkin
Matriculation Number: 01625804

# Timothy Atkin

Master Thesis supervised by
Univ.-Prof. Dipl.-Ing. Dr. mont. Gerhard Thonhauser
Dipl.-Ing. Asad Elmgerbi

# Numerical Modelling to Estimate the Amount of Formation Deformation and its Effect on Cement Integrity

**dpe DEPARTMENT PETROLEUM ENGINEERING**

**MONTAN UNIVERSITÄT**

*To Judith and my parents who supported me and gave me the idea to study in Leoben.*

# Abstract

In drilling, thus far, there have been several issues that may have significant impact on cement integrity that have not been fully understood. One of these issues is borehole ballooning. Borehole ballooning is sometimes referred to as breathing and is an expression used to describe the small volumetric change of the active fluid system, which might occur during the circulation of drilling fluids.

At the present time, there has been limited research and inclusion of cementing to the bore hole ballooning challenge. With the increased amount of focus that comes with well integrity issues, accurate prediction of borehole ballooning while performing primary cement jobs becomes increasingly necessary to assure that the volumetric change and its effect on the cement/formation bond that this causes is correctly accounted for.

In the context of the above challenges this thesis project aims to explore the utilisation of a numerical software model to study the effects of borehole ballooning that occurs while cementing on the cement integrity in terms of volumetric change, several scenarios are studied with three different types of cement and 3 different types of surrounding formation. Based on the results recommendations will be proposed, which may help to reduce risks and improve the cement operation.

This thesis suggests that a somewhat small volume change over a relatively moderate section length, as indicated by the results, could mean that problems with the integrity of wells might not be as considerable as originally proposed. This small volume would be taken into account by existing quantities of cement or by changing the cement properties in a minor way to reduce the degree of deformation. The strength of the surrounding formations also provides support and limits the amount of deformation. The displacement velocity has the largest impact on the level of deformation, the marginal difference increases as the velocity increases but is still comparatively small.

# Zusammenfassung

In der Bohrtechnik gab es bisher mehrere Probleme, die erhebliche Auswirkungen auf die Zementintegrität haben können und nicht vollständig verstanden wurden. Eines dieser Probleme ist das Balloning von Bohrlöchern. Bohrlochballoning wird manchmal als Atmung bezeichnet und ist ein Ausdruck, der verwendet wird, um die kleine volumetrische Änderung des aktiven Fluidsystems zu beschreiben, die während der Zirkulation von Bohrflüssigkeiten auftreten kann.

Gegenwärtig ist die Zementierung nur begrenzt in das Problem des Bohrlochballooning inkludiert und in diesem Zusammenhang untersucht worden. Mit dem zunehmenden Fokus auf die Integritätsproblematik von Bohrlöchern wird es immer wichtiger, eine genaue Vorhersage des Bohrlochballoonings bei der Durchführung des primären Zementiervorgangs zu treffen, um sicherzustellen, dass die volumetrische Änderung und ihre Auswirkungen auf die Zement / Formationsbindung, die dadurch verursacht wird, korrekt berücksichtigt werden.

Im Zusammenhang mit den oben genannten Herausforderungen zielt dieses Diplomarbeitsprojekt darauf ab, die Verwendung eines numerischen Softwaremodells zu untersuchen, um die Auswirkungen von Bohrlochballoning, das während des Zementierens auftritt, auf die Zementintegrität im Sinne einer Volumsänderung zu erfassen. Dabei werden mehrere Szenarien mit drei unterschiedlichen Arten von Zement und drei unterschiedlichen umgebenden Formationen untersucht. Basierend auf den Ergebnissen werden Empfehlungen vorgeschlagen, die dazu beitragen können, Risiken zu reduzieren und den Zementiervorgang zu verbessern.

Diese Arbeit kommt zu dem Schluss, dass eine eher kleine Volumenänderung über eine relativ moderate Abschnittslänge, wie die Ergebnisse zeigen, bedeuten könnte, dass Probleme mit der Integrität von Bohrungen möglicherweise nicht so erheblich sind wie ursprünglich gedacht. Dieses kleine Volumen würde durch vorhandene Zementmengen oder durch geringfügige Änderung der Zementeigenschaften berücksichtigt, um den Verformungsgrad zu verringern.

# Acknowledgements

Firstly I want to thank my thesis advisor Dipl.-Ing. Asad Elmgerbi from the University of Leoben for supporting and advising me over the duration of my thesis. He has always helped me, answering any questions I had when I was lost or stuck.

I want to thank Judith, my friends and family who supported me during my time of study and were always there for me in times of stress.

Finally, I also would like to thank all the employees and colleagues of the University of Leoben who helped to provide an excellent learning environment.

# Contents

# Chapter 1 Introduction

## 1.1. Overview

The formation deformation or borehole ballooning is sometimes referred to as breathing and is an expression used to describe the small volumetric changes downhole that affect the volume of the annulus, which might occur during the circulation of drilling fluids and or cement. With the increased amount of focus that comes with well integrity issues, accurate prediction of borehole ballooning while cementing becomes increasingly necessary to ensure that the volumetric change and its effect on the cement/formation bond that this causes is correctly accounted for.
This process could cause problems within the cement such as cracks forming in the cement and these joining together to form micro annuli. This amount of deformation occurs during the pumping of the cement

## 1.2. Motivation

Simulations and models are currently being used in the design of high temperature wells, wells with large cement volumes and long pumping times. In wells that have weak formations present, also that has narrow annular clearances. When a well is drilled in a new area or if that area is prone to gas migration and surface casing vent flows. Also, in problem drilling areas for example wells with a high level of deviation or are under/over pressured and finally in situations where new technology is being used. (Drilling and Completion Committee 2017)

An example of a standard approach to the cement design process can be seen in Figure 1. This approach is a basic outline of the standard design process. As read above the simulations or models which are carried out at the moment don't account for formation deformation and how this affects the cementing process.
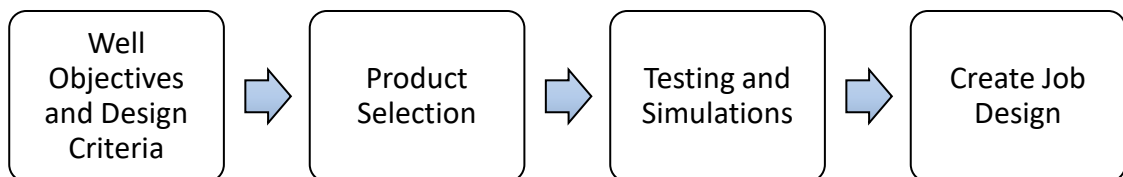
Figure 1. Typical Cement Design Process (Drilling and Completion Committee, 2017)

Since the Macondo accident in the Gulf of Mexico, a larger focus has been on cement integrity and therefore well integrity due to regulations from the state by using the correct amount and type of cement to fit the down hole environment.

## 1.3. Challenges

The main objective of the thesis is to investigate how the formation reacts to cement being pumped using standard procedures into the annulus in a prescribed environment that would only lead to load levels accurate for that setting. So different aspects of the proposed model will be studied, how the cement and the formation interact and how the different forces involved affect each other. This model that can be used in the case study will hopefully be able to provide a solution and ultimately help improve well integrity.

One of the key components of this approach is by utilising Ansys software and trying to incorporate as many parameters as possible to gain a meaningful result from the numerical model that hopefully will be created. This is challenging as it means using two parts of Ansys to work together, both the fluid simulation by using fluent and then the transient structural model to simulate the solid aspects. Linking the two simulations successfully in itself is a challenge that will hopefully be overcome.

Firstly, the objective which has been defined above will be abstracted and the physical phenomena described. Then the conservation laws will be applied through the Ansys software along with conservative relations and additional models, after this, the numerical method will be designed with the domain discretization and boundary conditions defined.

By using this model made up of a mixture of computational fluid dynamics, stress analysis and deformation a numerical model can be brought into being. Having imputed both the physical properties of the cement slurry in a known geometry and the stress regime and amount and rate of deformation of the surrounding formation and how this relationship affects the cement integrity over a fixed time period.

## 1.4. Objective

In this body of work, the plan is to confront the issue of well integrity from the point of view encapsulating formation deformation and cement integrity with the ultimate objective of this thesis project creating a numerical model to investigate cement integrity when performing a cement job and how formation deformation is affected. This model will try to consider:
- The geomechanical properties that are linked to the lithological properties of the rock, the mineral make-up and how the grains and or minerals are bound together. How this affects the strength of the rock and its elasticity.
- The in-situ stresses, which are related to the stress regime inherent in the earth.
- The formation temperature. This affects the fluid within the formation by altering its density and or the density of the fluid in the wellbore.

Then the model will also take into consideration the cement properties, for example:
- cement density,

The density of cement can range from 6 to 22 lb/gal. This depends on the chemical formula used to make up the cement and its internal components.

- viscosity,

The viscosity of the cement can vary; this also depends on the chemicals used and the cements components.

- strength,

The strength of the cement when it is set is down to the type of cement used and its properties.

With these two sets of properties which link the deformation of the formation with the cement, this relationship can be quantified so that the effect on the well's cement integrity can be analysed. Starting by analysing existing literature in a literature review and then develop a model which will then be applied to a case study with representative field data. The flow chart representing the processes behind this thesis is shown below in Figure 2.



**Theory**
- Examine formation Deformation
- Cement Design and integrity

**Model**
- Construction of the model
- Incorperating the model into a case study

**Results**
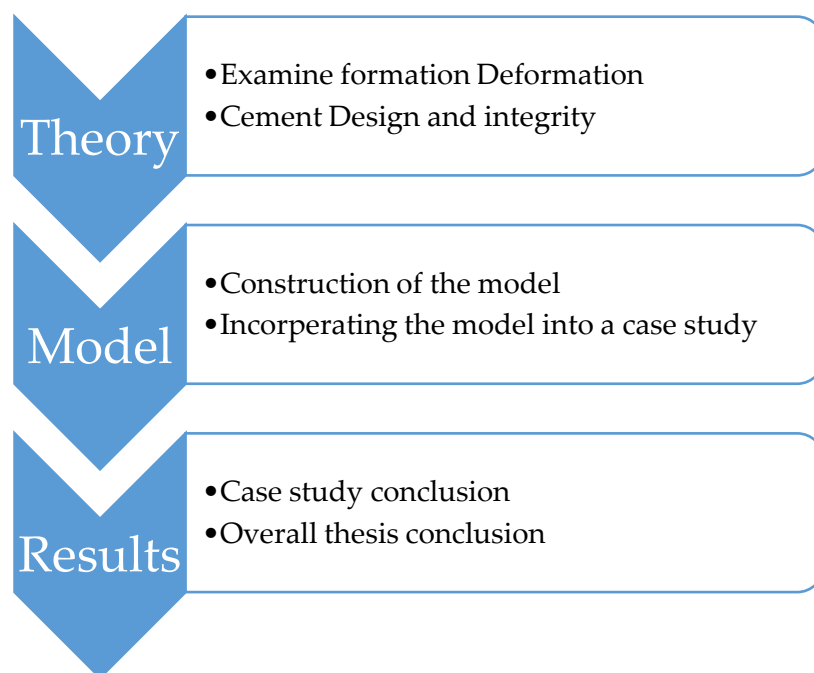- Case study conclusion
- Overall thesis conclusion

Figure 2. Process Flow Chart to Reach the Thesis Objective

# Chapter 2 Formation Deformation

## 2.1. Overview

Rocks in a geological setting are known as formations and are in a state of stress, which is mostly related to plate tectonics but is also due to the weight of overlying rocks also known as overburden their response to this stress is strain also known as deformation. In the regions close to where plates are converging the stress is typically compressive with the rocks being squeezed. Where plates are diverging the stress is extensive with the rocks being pulled apart. At transform plate boundaries plates are moving parallel to one another this causes a sideways or shear stress; this means that there the forces are acting in opposite directions parallel to a plane. Rocks have highly varying strain responses to stress because they have different compositions, both physical and mechanical properties, and also temperature has a large influence as geothermal temperatures within the crust can vary greatly. (Earle 2015)

The stress applied to a rock can be described by breaking it down into three dimensions with them all at right angles to one-another as seen in Figure 3. If the rock or formation is subject only to the pressure of burial from the overburden, then the stresses in all three directions will likely be the same. If the rock is subject to both burial and tectonic forces, then the pressures will be different in different directions. (Earle 2015)

The formation can react to stress in three ways: Firstly, it can deform elastically, it can then deform plastically, and it can also break or fracture. Elastic strain is reversible, so if the stress is removed, the rock will return to its original shape just like a rubber band that is stretched and released. Plastic strain, on the other hand, is not reversible. As already stated above different rocks at different temperatures can behave in different ways to stress. Higher temperatures lead to more of a plastic behaviour. Additionally, another factor that affects the strain in rocks and formations is the rate at which the stress is applied. If the stress is applied quickly for example, in the case of an extra-terrestrial impact or seismicity in the earth's crust causing earthquakes or artificially induced fractures from enhanced oil recovery, there is an increased tendency for the rock and the formation to fracture. Some of the different types of strain responses are illustrated in Figure 3. (Earle 2015)

The outcome from placing a formation under stress can be highly variable, but can include fracturing, tilting, folding, stretching, squeezing, and faulting. A fracture can be described as a simple break that does not have to involve significant movement of the rock on either side of the fracture. Natural Fracturing is particularly common in volcanic rock, which shrinks as it cools. (Earle 2015)

When a rock or a formation is compressed in one direction, it typically extends or stretches in another. This is an important notion because different formations and rocks are formed in varying stress environments. For example, limestone can be relatively easily deformed when heated, but another rock such as chert would remain

brittle, so if the formation would made up of chert and limestone, the limestone would stretch but the brittle chert would be forced to break into fragments to accommodate the change in shape of the whole formation.
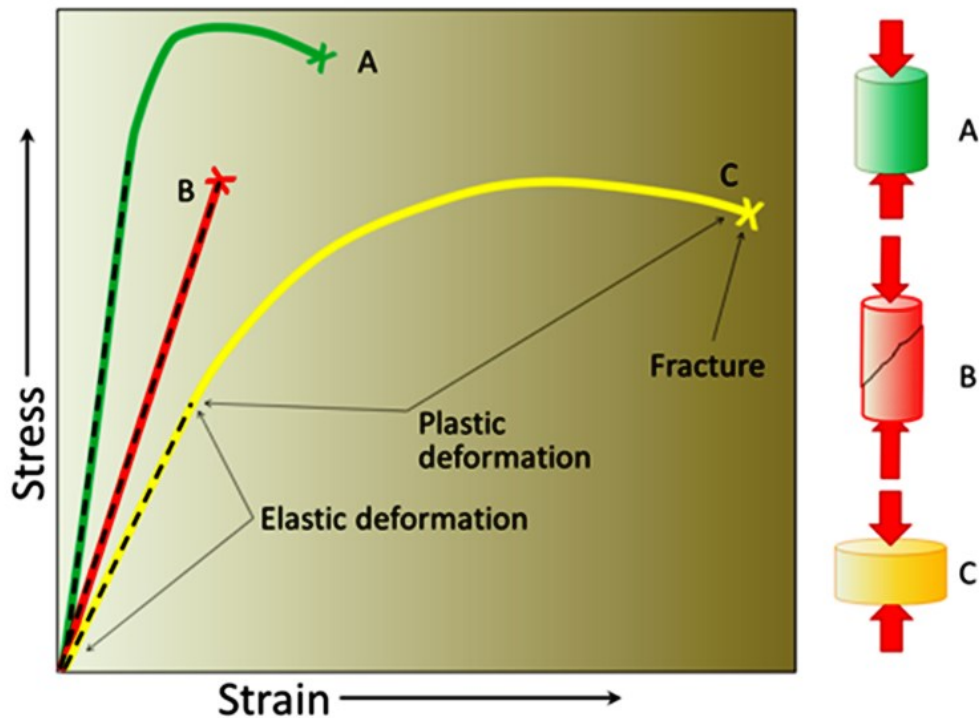


Figure 3. The Varying Types of Response of Geological Materials to Stress. (Earle 2015)

In Figure 3 the varying responses of geological materials to stress are visualized. The straight dashed lines are elastic strain and the curved parts are plastic strain. In each case, the X marks the point at which the material fractures. With A being the strongest material, deforms relatively little and breaks at a high stress level. The B material is strong but brittle, showing no plastic deformation and breaks after relatively little elastic deformation. The C material is the most deformable, breaking only after significant elastic and plastic strain. The three deformation diagrams on the right show A and C before breaking and B after breaking. (Earle 2015)

Formation deformation can occur during both drilling operations and cementing. When this occurs, it can cause a volumetric change in the active drilling fluid volume. However while cementing the impact of deformation may affect the cement integrity such as the interface between the formation and the cement itself, this is what this thesis will investigate. This change in volume is variable and depends on the well in question but can occur frequently.

Certainly, three processes can cause volumetric changes to the active drilling system; these processes are:

- Kick: A flow of formation fluids into the wellbore during drilling operations.
- Loss: The leakage of the liquid phase of a drilling fluid, slurry or treatment fluid containing solid particles into the formation matrix.
- Borehole breathing or Ballooning, this is covered below in greater detail as it encompasses a large part of this thesis as it is a part of formation deformation and is an effect that could become. (Elmgerbi, et al. 2016)

# 2.2. Borehole Breathing (Ballooning)

Borehole ballooning is the term used to describe reversible mud losses ad gains during drilling. The three main mechanisms are:

1. Thermal expansion and contraction of the drilling fluid.

This occurs due to the heat given off from the formations at depth along with the friction generated in the system while the well is being drilled. And this is then conducted through the drilling fluid as it is pumped around causing the fluid to expand. The contraction occurs when the mud cools down after the drilling has completed and the fluid is conducting the heat back into the formation.

2. Compressibility of the drilling fluid.

The compressibility varies with the fluid's composition and with the depth and hydrostatic and dynamic pressure acting on the fluid.

3. Elastic deformation of the borehole and the cased hole.

This is caused by the stresses inherently in the formations either as the hydrostatic, maximum, minimum stresses and areas of overpressure. This can be seen when while pumping the equivalent circulating density is greater than the strength of the elastic strength of the rock causing it to deform and then when the pumping stops the formation moves back close to its original orientation. (Lavrov and Tronvoll 2005)

4. The opening and closing of induced fractures at the near wellbore region.

The opening and closing of both natural and induced fractures occur during the same process but possibly at different pressures. The can occur when the drilling fluid density is too close to the fracture pressure and so when pumping the equivalent circulating density goes above that of the fracture pressure of the formation, this causes the fractures or already existing fractures to expand and then when the pumps have been turned off the fractures close again releasing drilling fluid back into the wellbore. A change in borehole volume due to elastic deformation can be significant and it is mainly driven by the wellbore radius, well pressure and Poisson's ratio. Their results show that the change in volume can be as high as 1 bbl. for 100 meters' depth interval. (Helstrup, et al. 2001)

The amount of formation elastic deformation and its effect on cement integrity can possibly cause problems that will have to be remediated in the future. As the main focus of this thesis is to identify the risks of deformation, the two statements below act as examples of what could happen and am required to investigate:

Cement cracking, as the cement hardens and the formation wall tries to return to a similar diameter after the expansion caused by the cement slurries ECD (equivalent circulating density), cracks can form along with micro annuli. This relates to gas migration which is covered in more detail in the next chapter.

The top of cement and the cement placement can be affected if the incorrect volume of cement and spacer is pumped. This can lead to unwanted formations being exposed to the borehole annulus affecting well integrity.

This trapped annulus pressure caused in the above situation can eventually allow communication of formation fluids to the surface. This trapped annulus pressure can be thermally induced or by sustained pressures. This will have to be taken into account in the well design to prevent the occurrence of excessive pressure that may have an impact on well integrity. (Norwegian University of Science and Technology 2012)

These well integrity issues can induce increases in non-productive time as remedial cement jobs and other operations will have to be carried out to rectify the foreseeable problems. As the cement has a higher density and rheology and a smaller annular gap between the casing and the open hole when cementing and as cementing equivalent circulating densities are higher than when drilling. It is widely believed that the worst-case scenario for inducing fluid losses in during cementing operations. Until the journal article by Therond, et al., 2018 little was know regarding the wellbore strengthening capabilities of cement sluries. The conclusion of this paper has clear evidence of losses and therefore deformation during cementing is actually reduced as it concludes that the cement increases the fracture strength of formations. (Therond, et al. 2018)

## 2.3. Elastic Deformation Estimation Methods

It is acknowledged that a borehole will alter the stress field around the hole, this means we must anticipate an adaptation in radial and circumferential stress concentration in and around the borehole wall. These equations first derived by Kirsch (1898) and describe the elastic stresses around the hole in a stressed infinite plate: (Al-Tahini and Abousleiman 2008)

$$\sigma_{rr} = \frac{\sigma}{2}\left[\left(1 - \frac{a^2}{r^2}\right) + \left(1 + \frac{3a^4}{r^4} - \frac{4a^2}{r^2}\right)cos2\theta\right] \tag{1}$$

$$\sigma_{\theta\theta} = \frac{\sigma}{2}\left[\left(1 + \frac{a^2}{r^2}\right) - \left(1 + \frac{3a^4}{r^4}\right)cos2\theta\right] \tag{2}$$

where $\sigma_{rr}$ and $\sigma_{\theta\theta}$ are the radial stress and circumferential stress elements. The angle $\theta$ regards to the far field compressive stress $\sigma$, the borehole radius is described by a and the distance to the borehole by r.

At the point where the borehole radius is at the maximum, r = a, the circumferential stress is highly compressive at the angles $\theta = 90°$ and $270°$, and tensile at $\theta = 0°$ and $180°$. That means, where the tangential compressive stress reaches a maximum, borehole failure and or breakouts arise. Failures at the borehole wall due to tensile stresses occur also when the stress concentration overcomes the tensile strength of the rock shown in Figure 4.
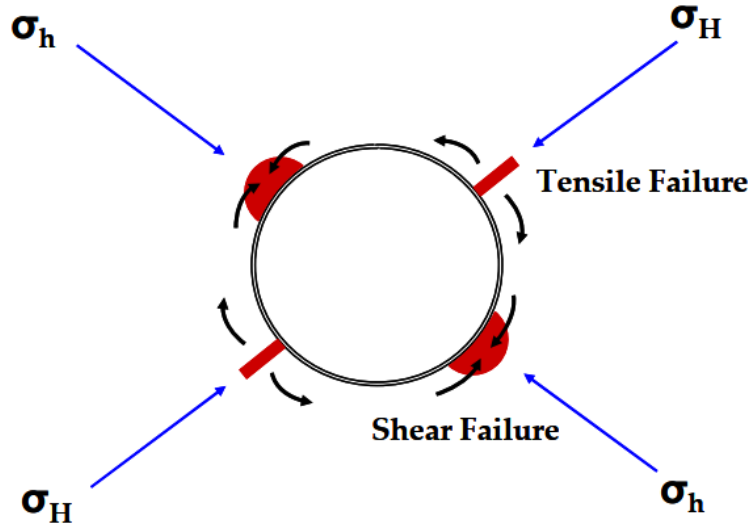
Figure 4. Borehole Failure due to Induced Stresses

Hooke's law of stress-strain relationships provides information about the borehole radial and circumferential strains, which can be followed back to the stress concentration around the borehole. This adjustment due to strain can be expressed in terms of stress as:

$$\varepsilon_{ij} = \frac{1}{E}\left((1+v)\sigma_{ij} - v\delta_{ij}\sigma_{kk}\right) \tag{3}$$

where E is the Young's modulus, v the Poisson's ratio and $\delta_{ij}$ is the Kronecker delta. The first two are elastic constants and the multiple indices indicate summation. (Al-Tahini and Abousleiman 2008)

The borehole displacements, in radial and tangential directions, u and v are expressed as:

$$u = \frac{1}{E}\left[\frac{\sigma}{2}\left(r+\frac{a^2}{r}\right) + \frac{\sigma}{2}\left(r+\frac{4a^2}{r}-\frac{a^4}{r^3}\right)\cos 2\theta\right] - \frac{v}{E}\left[\frac{\sigma}{2}\left(r-\frac{a^2}{r}\right) - \frac{\sigma}{2}\left(r-\frac{a^4}{r^3}\right)\cos 2\theta\right] \tag{4}$$

$$v = -\frac{1}{E}\left[\frac{\sigma}{2}\left(r+\frac{2a^2}{r}+\frac{a^4}{r^3}\right)\sin 2\theta\right] - \frac{v}{E}\left[\frac{\sigma}{2}\left(r-\frac{2a^2}{r}+\frac{a^4}{r^3}\right)\sin 2\theta\right] \tag{5}$$

The tangential strain component, $\varepsilon_{\theta\theta}$, which describes the alteration around the borehole can be expressed as:

$$\varepsilon_{\theta\theta} = \frac{\sigma}{E}(1 - 2\cos 2\theta) \tag{6}$$

Elastic deformation of a solid such as a geological formation can be estimated by using the method specified (Helstrup, et al. 2001) that a change in borehole volume due to elastic deformation might be significant and that it is mainly driven by the wellbore radius, well pressure and Poisson's ratio. This model was used for the drilling fluids and not cement.

Elastic deformation of a solid such as a geological formation can be estimated by using the method specified (Helstrup, et al. 2001) that a change in borehole volume due to elastic deformation might be significant and that it is mainly driven by the wellbore radius, well pressure and Poisson's ratio. This model was used for the drilling fluids and not cement.

Their method estimates that volumetric expansion can be based on analytical and numerical approaches. Analysis shows that the diametric expansion of the wellbore may be in the range of centimetres at a critical pressure, and therefore a deep well may consume a significant number of extra barrels of fluid before an actual breakout occurs. The results show that the change in volume could be as high as 1bbl for a 100m interval. (Helstrup, et al. 2001)

Bjørkevoll et al (1994) and Aadnøy (1996) studied two contributors to borehole ballooning, drilling fluid expansion, contraction and the elastic deformation of the borehole itself. They came up with the conclusion that a change in volume of the wellbore was mainly governed by the expansion and the contraction of the drilling fluid.

Then later Kåṙstad and Aadnøy (1996-1997) showed a method for calculating the elastic deformation of a borehole wall in order to correctly estimate the possible variation in volume of the wellbore. Although they did not consider the in-situ stresses in their method and they did not use precise rock properties like Young's modules. (Elmgerbi, Thonhauser, et al. 2016)

The introduction of an analytical formula for computing radial diametrical displacement of the borehole wall, with superimposed equations, with one for inward displacement and another second equation for outward displacement was carried out by Helstrup, et al. 2001. In order to validate their analytical solution, they compared the results with a numerical solution but their solution has some shortcomings.

They did not use realistic models for their comparison; the models should have been two dimensional as this makes for a better more accurate comparison. The numerical models used for the comparisons did not consider the poroelasticity theory. They assumed that the deformable areas would have a perfect elliptical shape and the solution ignored shear stresses. (Elmgerbi, Thonhauser, et al. 2016)

In 2008 Al-Tahini and Abousleiman performed experimental studies in order to ascertain a correlation between far field stresses with introduced stresses, displacement and breakout stresses. There are some shortcomings that can be taken away such as the uniaxial stresses used and the applied isotropic stresses, poroelasticity was also ignored and used rocks in their finite element simulation with no porosity, whereas their lab rock samples had porosity.

Then later in 2016 Elmgerbi, Thonhauser, et al. wrote a paper on estimating borehole deformation. The mathematical methods exposed before were adapted to estimate the deformation area for a given depth. It provided a practical concept to determine the

volumetric change of an open borehole that has been comprehensively described. A sensitivity study was carried out that demonstrated that the volumetric change of the borehole due to elastic deformation was volatile and was mainly controlled by the fluids weight and the borehole temperature and with the final result being that the deformation was not significant when taken into account individually. (Elmgerbi, Thonhauser, et al. 2016)

# Chapter 3 Cement Design and Integrity

The objective of primary cementing is to provide zonal isolation. Cementing is the process of mixing slurry of cement, cement additives and water and pumping it down through the casing to critical points in the annulus around the casing or in the open hole below the casing string. The four principal functions of cementing in a borehole are:

- To restrict fluid movement between the formations
- To bond and support the casing and also protects against corrosion
- To have a short waiting on cement time which helps prevent blow outs
- To protect the casing from shock loads caused by deeper drilling

## 3.1. Fundamentals of Cement Properties

To fulfil the mentioned functions above, there are several properties that have to be taken into account. These are listed in the following subsections:

1. Compressive strength: The compressive strength is the function of temperature, pressure, mix water amount and the time elapsed.
2. Thickening time or Pumpability: This is the time during which the cement is being pumped. The cement needs a significant time to be mixed, pumped and be displaced to the right position.
3. Water loss: pumpability decreases with fluid loss with primary pumping not as critical on fluid loss.
4. Corrosion resistance: Can cause deterioration of the cement sheath for example if sodium sulphate or magnesium sulphate react with the lime and other parts of the cement to form calcium sulpha laminate, this can cause cracks.
5. Permeability: After hardening the permeability will be very low (<0.1 millidarcies), if the cementing process is not carried out correctly then there is the possibility of channels forming (5-10 darcies)
6. Density: can be altered to meet operational requirements and is found in more detail in the following subsection.

## 3.2. Density

To maintain the integrity of the wellbore, the hydrostatic pressure exerted by the cement, drilling fluid, etc. must not exceed the fracture pressure of the weakest formation. The fracture pressure is the upper safe pressure limitation of the formation before the formation breaks down (the pressure necessary to extend the formation's fractures). The hydrostatic pressure of the fluid in the wellbore, along with the friction pressures created by the fluid movement, cannot exceed the fracture pressure, or the formation will break down. If the formation does break down, the formation is no

longer controlled and lost circulation results. Lost circulation, or fluid loss, must be controlled for successful primary cementing. Pressures experienced in the wellbore also affect the strength development of the cement

Controlling the cement slurry density is critical for placing a column of cement where the formation may be fractured by a heavy slurry or would allow the well to flow if the cement slurry was lighter than the pore pressure. For a lighter weight cement than the normal 15 to 16 Ib/gal, bentonite clay may be added to absorb water to yield a lighter cement with higher bound water volume. 10 to 12 Ib/gal cement density can be achieved in this way.

Grinding the cement to a very small size will also require more water to satisfy the high surface area and lighten the slurry to the 10 to 12 Ib/gal range. Ultra-light-weight cements, 6-7 using hollow ceramic or glass beads can reduce the overall weight of the cement slurry to less than 9 lb/gal. Even lower densities can be achieved by foaming the cement with a compressed gas such as nitrogen bubble.

The foamed cements can create densities of 4 to 7 lb/gal but require careful control of annulus surface pressures to avoid gas channels and voids. All these light weight cements, although strong enough to support the pipe, have less strength than the regular Portland cement.

Heavy weight materials are added to the cement to increase the cement density, usually to control the pressure in the formation during the pumping of the cement. Iron ore, barite (barium sulphate) and sand can create slurries to 25 lb/gal.

Other methods of preparing heavy weight slurries include the use of dispersants which allow less water to be used in cement and still maintain pump ability. A chart of cement density for various methods of density control is contained in the table below.

| Cement Slurry Type | Weight Range (lb/gal) | Specific Gravity (sg) |
|---|---|---|
| Densified and weighted | 16 - 22 | 1.9 – 2.6 |
| Neat Slurry | 14 - 18 | 1.6 – 2.1 |
| High water ratio slurries | 11 - 15 | 1.3 – 1.8 |
| Ceramic bead extended slurry | 9.5 - 12+ | 1.1 – 1.4+ |
| Glass bubble extended slurry | 7.5 - 12+ | 0.9 – 1.4+ |
| Foam cement | 6 - 12+ | 0.7 – 1.4+ |

Table 1. Cement Types and Density/weight range (George E King Consulting 2011)

Having an incorrect cement density can cause gas migration, poor set strength, inadequate cement bond, blow outs, formation fracturing and lack of mud displacement.
Cement slurry density must be rigorously controlled to enable the subsequent well completion steps to be carried out successfully. Also cementing in deep water wells has additional problems, with long thickening times needed and therefore slow compressive strength development, this can also lead to unpredictable gel strength
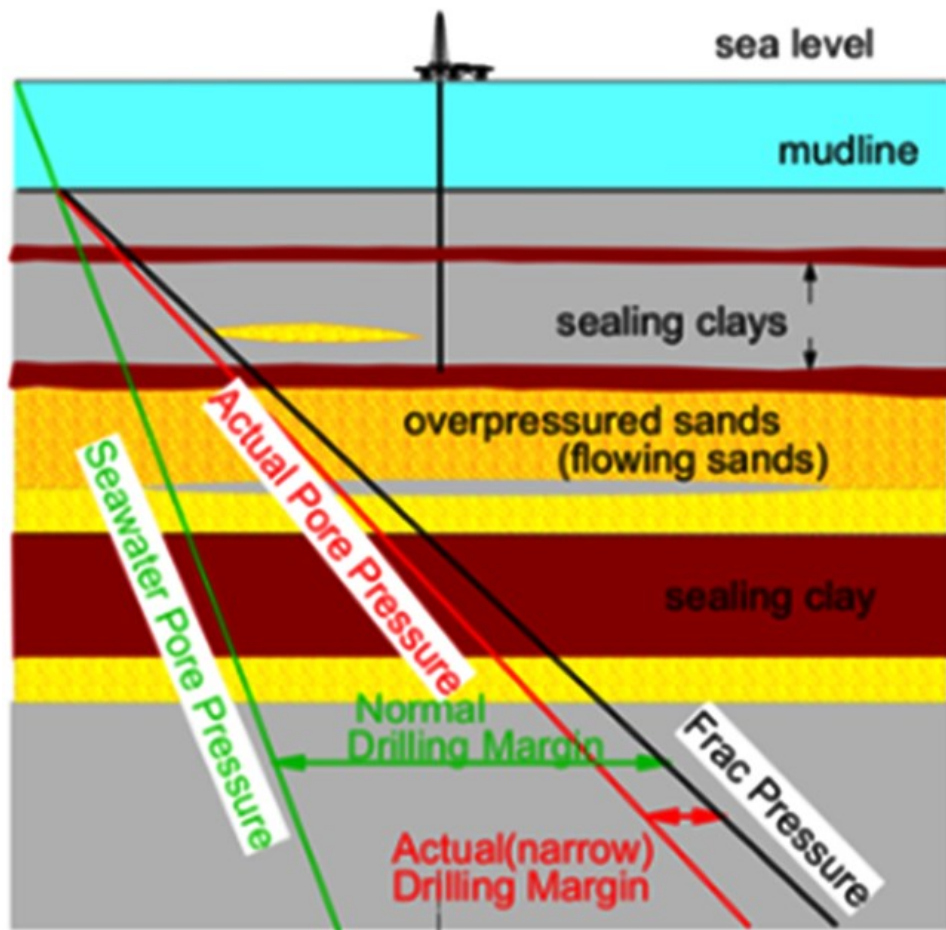
development. (Hagura 2003)



Figure 5. Typical deep-water Pressure Gradient (Hagura 2003)

## 3.3. Cement Additives

Cement additives are typically known by their trade names and are used to vary slurry density, change the compressive strength, accelerate or increase the setting time, control filtration and fluid loss and reduce slurry viscosity. They are blended with the cement powder or added to the mix water before mixing.

### 3.3.1 Accelerators

Accelerators shorten the time cement is set; this can be important in shallow wells so that the waiting time is not to large. The common types are calcium chloride and sodium chloride. In higher than 1.5 to 2.5% they can begin to act as retarders.

### 3.3.2 Retarders

With higher temperatures in deep wells, this reduces slurry thickening times so to prolong this thickening time retarders have to be used the most common types are calcium lignosulphonate and saturated salt solutions.

### 3.3.3 Light Weight Additives or Extenders

These reduce the density of the slurry and increase the thickening time and increase the amount of slurry produced from each cement sack. The common types are:
- Bentonite, absorbs water allowing more mix water to be added, reduces the strength of the cement and the sulphate resistance
- Pozzolan, used in 50/50 with mix with Portland cement, decreasing the strength and increases sulphate resistance
- Diatomaceous earth, large surface areas, allows more water absorption, low density slurries of 11ppg

### 3.3.4 Heavy Weight Additives

These are applied normally in over pressured zones to increase the cement density:
- Barite, densities up to 18ppg, reduces strength and pumpability
- Haematite, densities up to 22ppg, reduces pumpability
- Sand gives a density boost of 2ppg

### 3.3.5 Fluid Loss Additives

Fluid loss additives prevent dehydration and premature setting and are commonly made of either organic polymers (cellulose) or carboxymethyl hydroxyethyl cellulose (CMHEC) which can also act as retarder.

### 3.3.6 Friction Reducing Additives (Dispersants)

Improve the flow properties of the slurry, lowering the viscosity. This can help reduce the risk of formation breakdown. They can be made up of polymers, salt or calcium lignosulphonate.

### 3.3.7 Mud Contaminants

Can in some cases improve the slurry properties, but mostly reduce the given desired properties of the cement. This is combated by using a spacer fluid to help prevent contamination. These contaminants can have the following effects:
- Barite: increases the cement density and reduces the compressive strength
- Caustic acts as an accelerator
- Calcium compounds decrease the density
- Diesel oil – decreases density

## 3.4. Mechanism for Fluid/Gas Migration in the Cement

During this process hydrostatic pressure is key because while cementing the cement ensures that the pore pressure is below the wellbore pressure and therefore there is no invasion of fluids from the formation surrounding the borehole. After placement cement loses its ability to transmit the hydrostatic pressure due to the cement's static gel strength causes a deterioration in hydrostatic pressure transmission. This can cause knock on effects such as changes in downhole volumes, temperature, fluid loss and or

hydration volume reduction. The consequence of this is that the pore pressure within the gelling cement decrease and therefore becomes smaller than the formation pore pressure which makes it possible for gas or water to invade the annulus. (Hagura 2003)
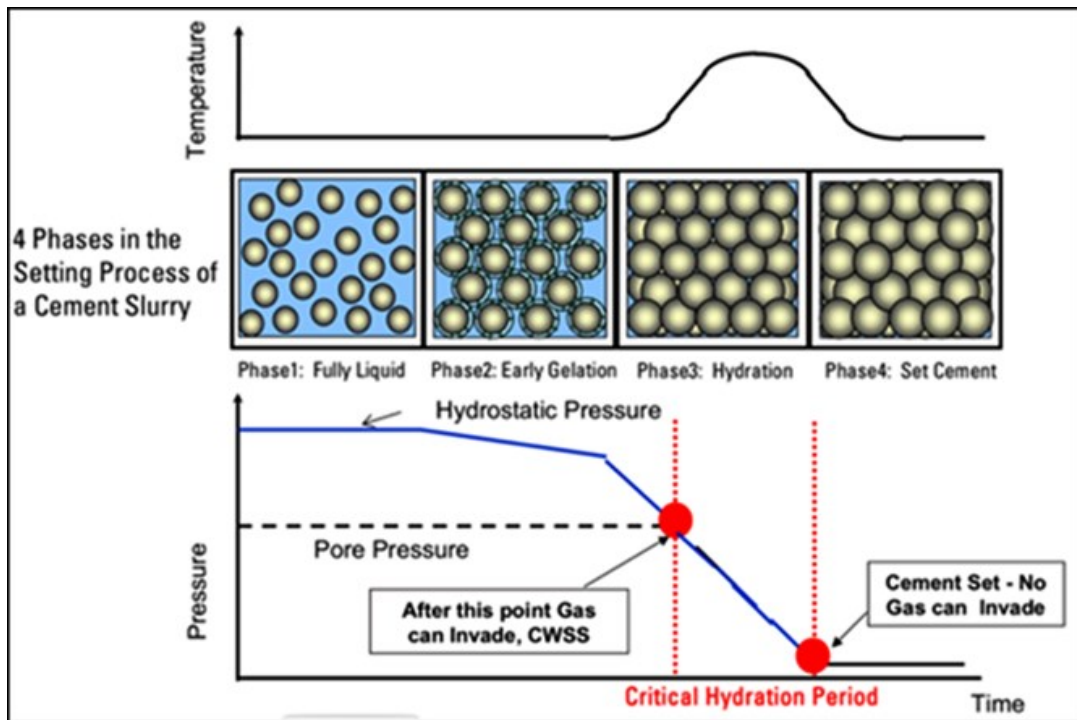


Figure 6. Gas or Fluid Invasion in Setting Cement (Hagura 2003)

In Figure 6 which shows the possibility of gas or fluid invasion in cement, static gel strength or SGS is a measure of attractive forces between particles of a fluid under static conditions. The measure of the attractive forces of a fluid under dynamic or flowing conditions is what is commonly referred to as the yield point of the slurry.

When the hydrostatic pressure dropped to the level of the pore pressure, there is a point known as the critical wall shear stress (CWSS). This is a measure of the amount of gel strength that must develop to cause hydrostatic deterioration and a allow gas entry. This is not a property of the cement slurry, so this is totally dependent on the well geometry and pressure.

$$CWSS = 0.25 \left[\Sigma(\rho_x g L_x \cos\Theta) - P_f\right] [D_h - D_c] / L_{cmt} \text{ where:}$$



where:

$\rho$ = fluid density
$g$ = gravity
$L$ = length of column
$\Theta$ = angle of inclination
$P_f$ = pore pressure
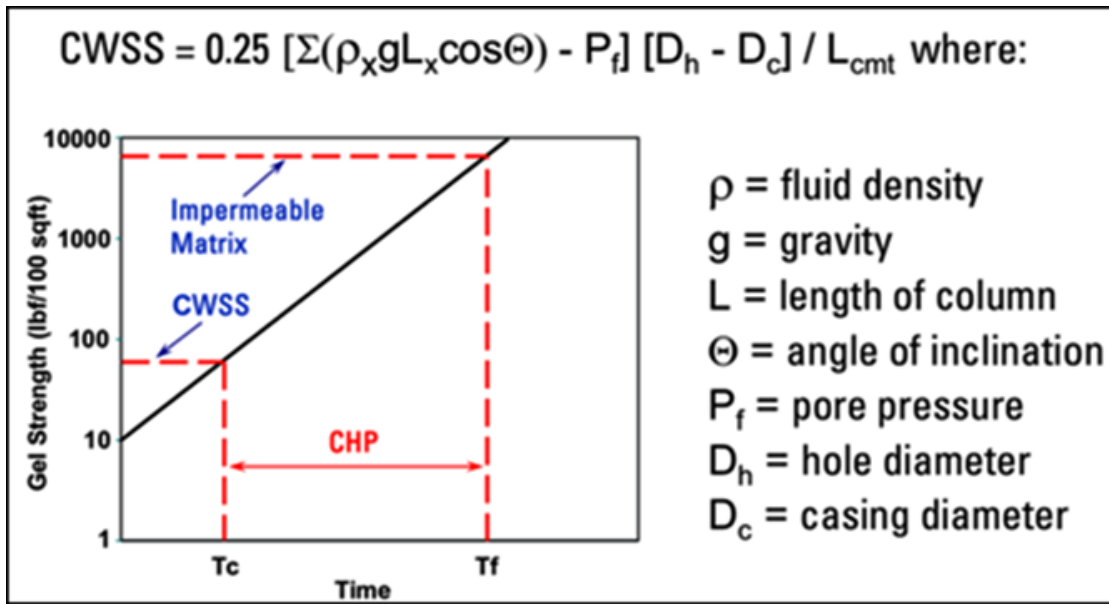$D_h$ = hole diameter
$D_c$ = casing diameter

Figure 7. Critical Hydration Period (Hagura 2003)

Then once the slurry has reached the critical hydration period (CHP) this is the point where the cement is set, and no further invasion can occur as described in Figure 7. This describes the gel strength development over time. In Figure 8 the CHP is adjusted by adding additives to speed up the gel strengthening process. This would improve the chance of providing a good seal against an influx.
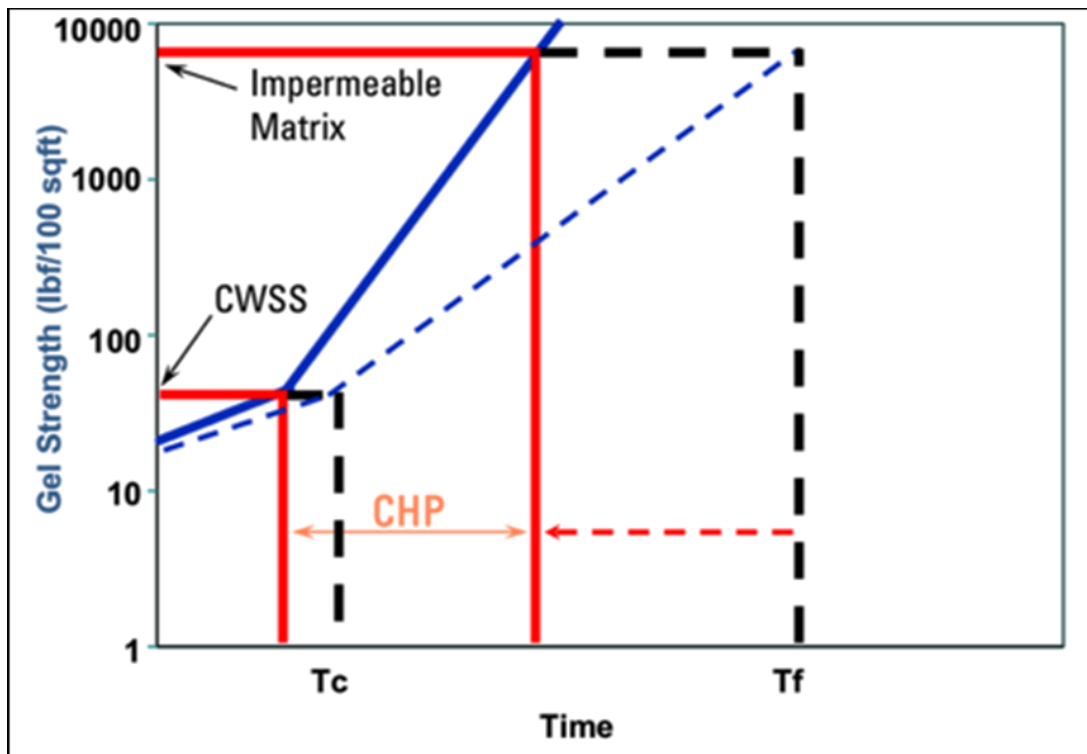


Figure 8. Reducing CHP by Slope Change of Static Gel Strength (Hagura 2003)

Zonal isolation is not directly related to production; however, this necessary task must be performed effectively to allow production or stimulation operations to be conducted. The success of a well depends on this primary operation.

Remedial cementing as it is usually done to correct problems associated with the primary cement job. The need for remedial cementing to restore a well's operation indicates that primary operational planning and execution were ineffective, resulting in costly repair operations. Remedial cementing operations consist of two broad categories, Squeeze and Plug cementing. Both are correction processes which should be avoided if possible, by performing an adequate primary cement job.

## 3.5. Cement Design Process

In general, there are four steps required to successfully plan and place cement in the wellbore to fulfil the principal functions previously outlined. Firstly, the well parameters need to be analysed so that the needs of the well are met. Then the composition of the cement is designed to meet the needs for the whole life of the well. The cement slurry composition has to be tested, so they meet the well parameters set out. These fluid parameters can then be adjusted to better fit the design scenario. Then the cement job itself is designed. So how the cement will reach its final destination in the wellbore.
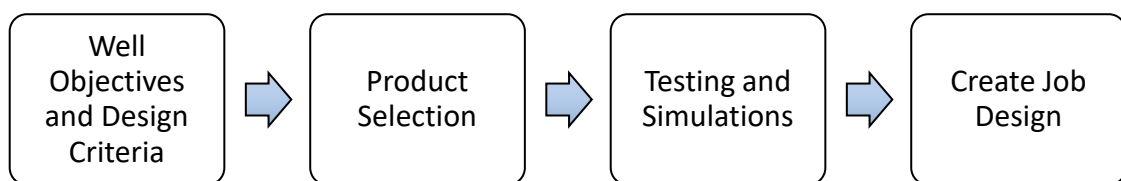
Well Objectives and Design Criteria → Product Selection → Testing and Simulations → Create Job Design

Figure 9. Typical Cement Design Process (Drilling and Completion Committee 2017)

### 3.5.1 Well Objectives

The well objectives are based on the trajectory, depth, geological formations wanting to be reached, etc.
So the cementing design criteria has to fit into these objectives, to fit in with the drilling and casing objectives and also fulfil the four principal functions as stated at the beginning of this chapter.

### 3.5.2 Product selection

Based on the well objectives the products for the scenario can be selected to fulfil the correct property specification using the correct types of additives as stated above in the right quantities and the cement mix strategy to best create the cement slurry.

### 3.5.3 Testing and Simulations

Simulators are typically used in the following situations:
- High temperature wells
- Large cement volumes
- Long pumping times

- Weak formations
- Narrow annular clearances
- New areas for drilling
- Areas prone to gas migration and surface casing vent flows
- Problem drilling areas (e.g., high deviation or over/under pressured)
- New technology is being used (e.g., monobores)

(Drilling and Completion Committee 2017)

Simulators can calculate the predicted surface pressures, rates and equivalent circulating density (ECD) throughout the cementing process as well as final placement of all fluid pumped into the well during the cementing job. Other outputs from the simulator may include the cementing and spacer volumes, hook load calculations, centralizer spacing calculations, also free fall calculations and the flow regimes encountered during the cement job. The casing collapse and burst calculations and also foam cement calculations and finally gas flow potential calculations.

Well and fluid information are needed to complete a simulation. The accuracy of the simulation is dependent on the quality of the data used as an input. It is important for the operator and cementing service provider to work together to ensure the required data is made available in order to limit any assumptions.

There are a few inputs that are typically used basic simulations; these are depths, wellbore dimensions, formation pressures, fracture gradients, pipe dimensions, directional survey information and also accurate calliper measurements. The temperature gradients of the well and also the position of lost circulation zones. The cement slurry properties such as density and rheology. The pumping schedule such as fluid volumes and rates. This input data is imported into the simulation software to compare the job design with actual parameters. This will help in the verification process to quantify the success of the cementing operation and feed into a continuous improvement cycle for the overall cementing process. (Drilling and Completion Committee 2017)

In literature, there have been no other serious methods for a numerical model for cementing in this environment and how formation deformation and ballooning affects this. Only during drilling, this idea has been entertained to monitor for losses and kicks, so if this model can be adapted, then it would help fit. In the context of the above challenges, this project aims to explore the utilisation of numerical software model to study the effects of borehole ballooning that occurs while cementing and its effect on the cement integrity

### 3.5.4 Create Job Design

The job design is based on the above well objectives, products selected and simulations carried out. Then the way the cement will be pumped is selected so done in one stage, two stages or multi stage. The height of the cement sheath has to be chosen and according to governmental regulations and well integrity how high the top for the cement should be either to surface or a given distance above a troublesome formation.

# Chapter 4 Simulation Methodology

## 4.1. Overview

While cementing it is thought that the rock deformation should be greater due to the higher density of cement than the drilling fluid and a smaller annular gap between the pipe and the open hole than when drilling with drilling fluid, as equivalent circulating densities (ECD) are generally higher for cementing than for drilling. The possible formation deformation and volumetric changes could lead to ineffective zonal isolation and costly well repair.

The goal of this chapter is to create a working model to address the issues mentioned above and will be confronted by using Ansys fluent and Transient structural models to be used in the case study later in this thesis. This is done by understanding how the software works and bringing together the equations that are working in the background and to apply them to a given geometry and mesh.

The simulation methodology that will be followed is illustrated in the diagram below. The process begins with a problem which is then undergoes abstraction to come up with the abstracted problem. Then the modelling can begin with the mesh being created along with conservation laws and conservative relations defined. During Pre-processing the numerical method and boundary conditions are defined and domain discretization is carried out, this makes up the discretized model. The numerical algorithms are then run to come up with a solution. This solution is then validated, and the problem is refined and then the whole process is run through again until the solution is valid and within a well-defined error. This solution can then be processed. More details about the background behind the software can be found in the Appendix.
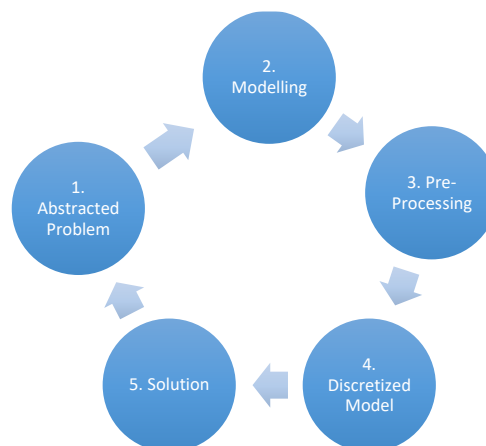


Figure 10. Modelling Process

# 4.2. Simulation Setup

The setup of the simulations began with choosing the types of simulations that were needed to fit the scenario. The Fluent simulation was chosen to simulate the flow of the cement ,then with a second simulation using the result of the fluent simulation to apply the pressure results to the solid formation surrounding the annulus. This is so that the 2 parts of the model can be studied simultaneously, the slurry flow and the cement and the surrounding rock. This setup is covered in greater detail in the following subsection and is illustrated in figures 11 to 14.

## 4.2.1. Ansys Fluent Parameters for 3D Multiphase Fluid

For the multiphase fluid model part of the simulation, as mentioned before, Fluent was chosen as the simulator for this model. This simulator is split in its setup into the model itself, so the geometry and mesh. This is followed by the simulation setup, solution and finally the results.
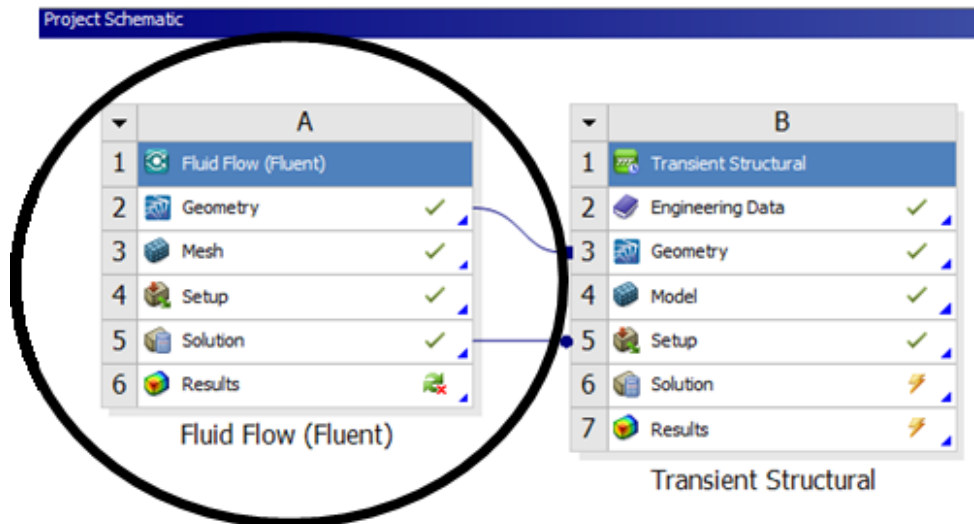


Figure 11. Fluent Project Structure

### 4.2.1.1. Model

Figure 11 displays the engineering project page from the Ansys workbench; this is where models are designed and created. This structure shows the geometry is shared between the two models and also the results from fluent going into the setup of the transient structural model.

### 4.2.1.2. Geometry

For the purpose of the simulation, a geometrical model of the flow domain was created based on actual well data. The geometry consists of the casing and annulus for a 0.5 m section of a well was set at a cube of 50x50x50cm with borehole through the middle of 12.25" hole and a casing outer diameter of 8.5". The geometry has an annular space of 0.72".

The geometry was created in Space Claim which is part of the Ansys design software. For the geometry to be recognized as actual flow domain by Fluent, it has to be completely watertight, which means that the elements of the model are solid shapes without openings in the outer surfaces. The geometry can be seen in Figure 11. The separate parts of the geometry are separated by material type. The rock (sandstone, limestone and dolomite), the fluid zone which is made of the drilling fluid and cement and the casing which is set up as a fixed wall.
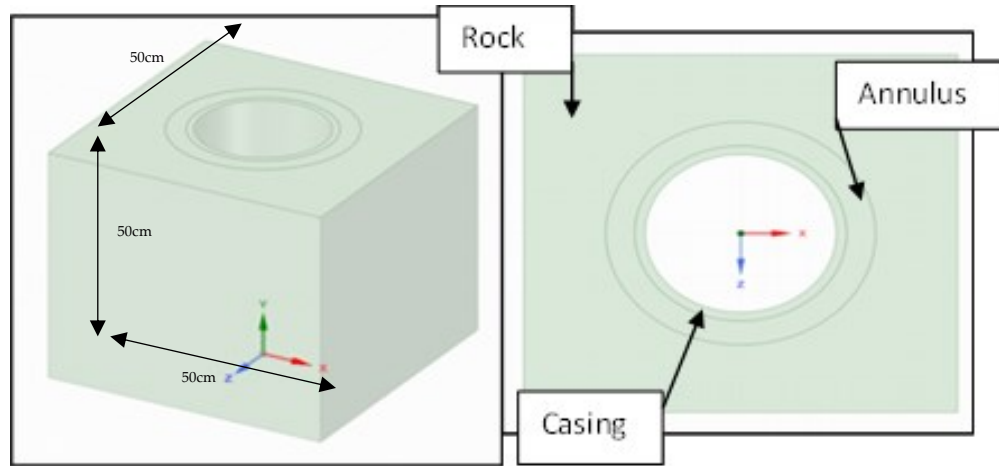


Figure 12. Geometry of the Model in 3D and Also As 2D Vertical View

## 4.2.1.3. Mesh

In the meshing process, the watertight geometry of the flow domain is discretized into computational cells necessary for the subsequent simulation. This process is done automatically by the meshing tool. The meshing tool has a variety of input parameters that control the meshing process such as the cell size. For the purpose of this simulation, the goal was to have the model meshed in a sufficiently high resolution to show the intended flow phenomena. Using the global coordinate system and connections between the 3 separate bodies (fluid, casing and rock) defined the mesh can be created.

A multi zone mesh was used as this provides the best flexibility and fits with the multiphase flow that occurs in the fluid zone. The mesh is of a Hexahedral type with edge sizing on the inlet and outlet edges and face meshing on the face of the inlet and outlet; this can be seen in Figure 13.
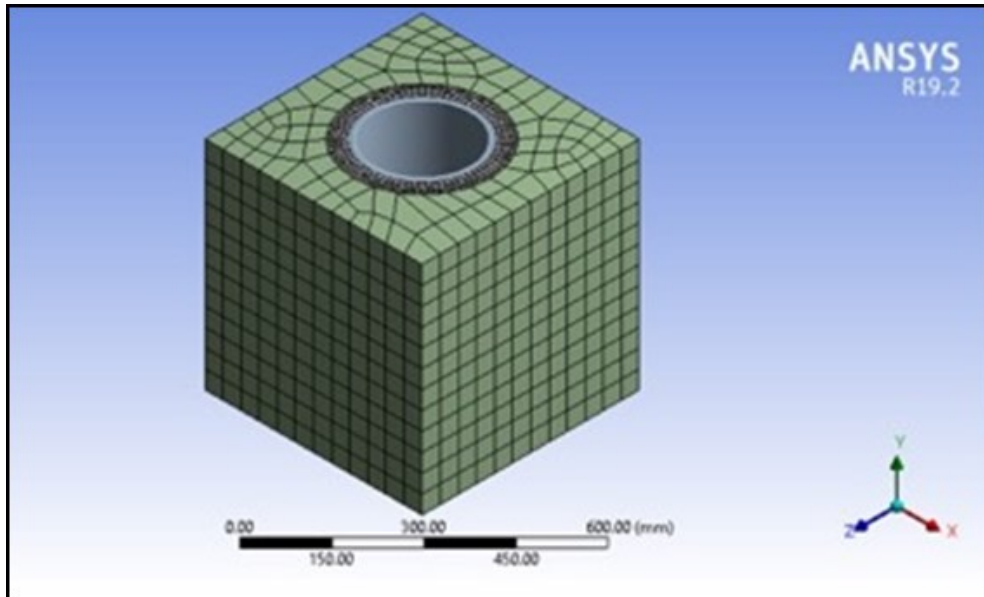
Figure 13. Mesh Structure for 3D Geometry

In Figure 14 the formation was meshed with a total of 14801 nodes and 11168 elements using multizone method with a hexahedron mesh type. The mesh structure for the fluid geometry below was set to a very fine mesh of program-controlled hexahedron cells in a multi zone method. The mesh had a total number of 9920 elements and 13020 nodes.
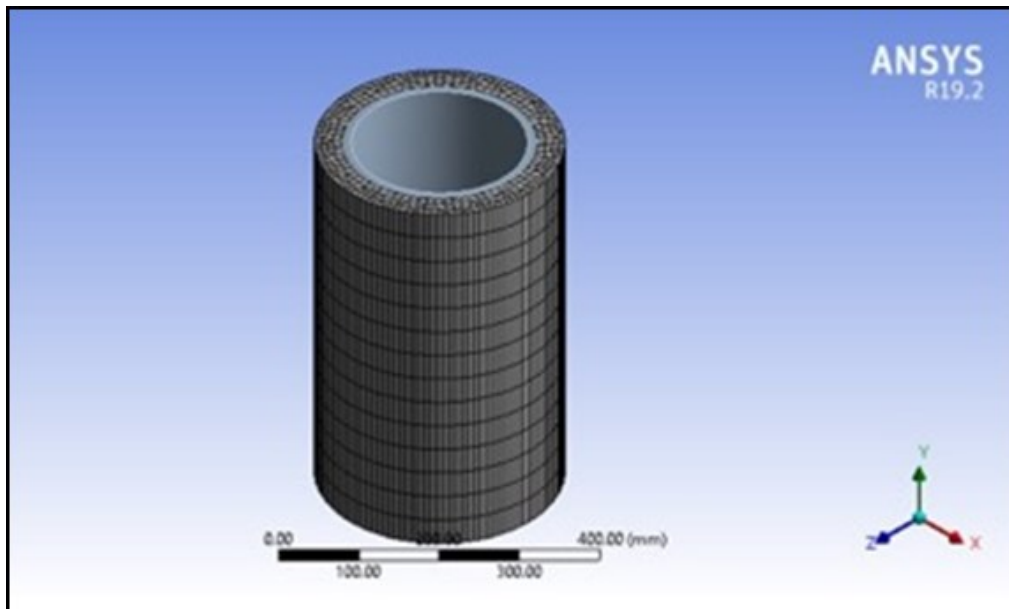


Figure 14. Mesh Used in the Fluid Geometry

## 4.2.2. Ansys Transient Structural Mechanical Parameters for 3D Multiphase Fluid Model

The transient structural part of the Ansys workbench is displayed in the black circle in Figure 15. These blue lines in between represent the information transferred between the two models. The first blue line is the geometrical information and the second is the fluent solution being transferred and imported into the setup of the transient structural model. The engineering data section of the transient structural model is where the materials can be set up or chosen from the Ansys materials library. The properties of the materials are fully adaptable with different properties being selected based on their application.
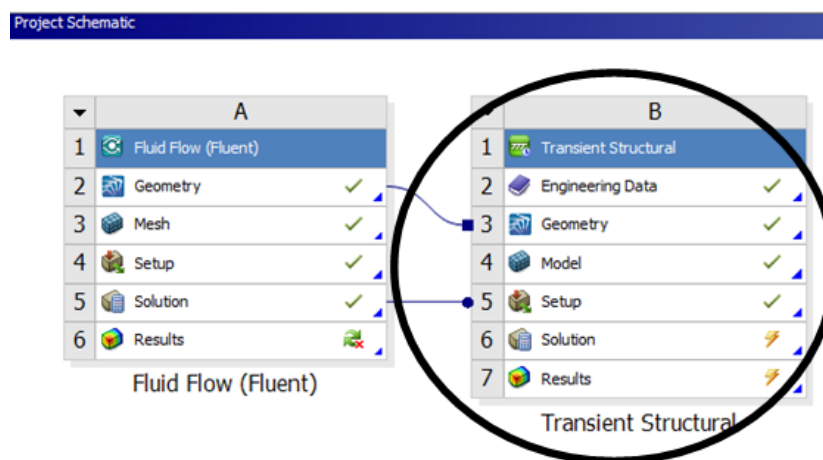


Figure 15. Transient Structural Mechanical Project Overview

The geometry, mesh and materials are the same that is used in the Fluent model. There are two contact regions, one between the fluid zone and casing and the other between the fluid zone and the sandstone rock.

# 4.3. Pre-processing

For the modelling process a paper from Therond, et al., 2018 was used as a base case to build the model upon. This paper contains the results of a field analysis performed to understand the stat of lost circulation during different phases of drilling and primary cementing in offshore wells. Four different locations were used in the study, the Gulf of Mexico, UK, Angola and Azerbaijan. Then in parrallel laboratory research was performed to understand the behaviour of cement slurries in different loss circulation scenarios. The objective of this study was to understand twhen lost circulation starts during a cementing operation and how wellbore mechanisms apply to cementing fluids. (Therond, et al. 2018)

The base data for this study will be used in the study of this thesis, using the same material properties of both the cement described and also the cement developed and

described which is specifically developed to fit this kind of environment stated by Hagura, 2003. The parameters that are going to be focused on and considered are:

| *Variable* | *Assumptions* |
|---|---|
| Cement density | Depth (TVD) |
| Viscosity of cement | Permeability of the test formation |
| Flow velocity | Formation temperature |
| | Porosity |
| | Pore pressure |
| | Formation strength |
| | Drilling Fluid density |
| | Viscosity of Drilling Fluid |
| | Rheology of Drilling Fluid |
| | Volume of each fluid |

Table 2. Variables and Assumptions for simulation models

These parameters will be applied to a defined scenario which would have the properties of an environment prone to deformation. For example, an environment which when circulating the drilling fluid, the equivalent circulating density exceeds the fracture pressure of the formation and when there is no circulation of drilling fluid, the equivalent static density is less than the pore pressure. This kind of environment occurs in wells that are in deep water usually or are abnormally stressed.

## 4.3.1.    Boundary Conditions

### 4.3.1.1.    Velocity Inlets

The velocity properties of flow at the inlet boundary are defined and are intended for incompressible flows. The properties of flow are not fixed and vary to accommodate the prescribed velocity distribution.

### 4.3.1.2.    Outflow Boundary

Outflow boundary conditions are used to model where the flow exits the model. The details of the flow velocity and pressure are not known prior to solution of the flow problem.

Appropriate to where the exit flow is close to a fully developed condition, as the outflow boundary condition assumes a zero-normal gradient for all flow variables except pressure. The solver extrapolates the required information from the interior of the flow domain and then an overall mass balance correction is applied.

Wall boundary condition are used to bound the fluid and solid regions. In viscous flows, no-slip conditions are enforced at the walls. Normal velocity component is set to be zero. Alternatively, the shear stress can be specified.

### 4.3.1.3.    Thermal Boundary Condition

Several types are available, Wall material and thickness can be defined for 1-D or in-plane thin plate heat transfer calculations. Wall roughness can be defined for turbulent flows.  Wall shear stress and heat transfer based on local flow field.

### 4.3.1.4.    Cell Zones for Fluid

A fluid zone or flow domain is the group of cells for which all active equations are solved. A Fluid material input required. Optional inputs allow the setting of source terms such as Mass, momentum, energy, etc.
The fluid zone can be defined as laminar flow region if modelling transitional flow. The zone can also be defined as porous media. The fluid motion can also be defined for the fluid zone.

### 4.3.1.5.    Porous Media Conditions

Porous zone modelled as a special type of fluid zone but isn't used in this case.

### 4.3.1.6.    Cell Zones for Solid

A solid zone is a group of cells for which only heat conduction is solved, and no flow equations are solved in fluent. The material being treated as solid may actually be fluid, but it is assumed that no convection takes place. The only required input is material type so that appropriate material properties are being used. Optional inputs allow you to set a volumetric heat generation rate (heat source).

### 4.3.1.7.    Internal Face Boundaries

These are defined on cell faces. They do not have a finite thickness and provides a means for introducing a step change in flow. The internal face boundaries are used to implement physical models that represent; fans, radiators, Porous jumps and interior walls, also known as thin walls.

### 4.3.1.8.    Material Properties

For each zone, a material needs to be specified. For all materials, the relevant properties need to be specified, such as density, viscosity, molecular weight, thermal conductivity, diffusion coefficients.
The properties that need to be specified depend on the model. Not all properties are required. For mixtures, for example, properties may have to be specified as a function of the mixture composition.

## 4.4.  Processing

This three-dimensional model created in pre-processing and instead of just using Ansys Fluent the model was incorporated with the Ansys transient Structural module. The geometry used can be seen in Figure 15. The model was then developed so that the

fluid ahead of the cement, the drilling fluid was also considered with regards to hydrostatic pressure and their chemical properties as seen later in the chapter 5.

In order to obtain positive simulation outcomes, the correct settings in the simulation software need to be chosen. It can be challenging to decide which models and particular settings to use. Typically, this kind of understanding comes with extensive knowledge of the simulator and with fluid dynamics in general. For the following case study, a number of practice runs were made to help decide on the correct settings for this situation.

For this study a two-phase cement – drilling mud flow was chosen as the flow regime. In CFD studies it is important to understand what flow regimes to expect in order to set up the software with the proper models as not all models are made for all flow regimes.

For this thesis the VOF model was chosen as it handles free – surface flows with the lowest computational needs. "The VOF model is a surface-tracking technique applied to a fixed Eulerian mesh. It is designed for two or more immiscible fluids where the position of the interface between the fluids is of interest. In the VOF model, a single set of momentum equations is shared by the fluids, and the volume fraction of each of the fluids in each computational cell is tracked throughout the domain" (Fluent Inc. 2006).

Fluent has two separate types of solvers which can be used, and each have their individual pros and cons, these are:
• Pressure – based
• Density – based

For this thesis, a pressure-based solver has been used as it is generally more precise than a density-based solver for subsonic flows. The velocity field is obtained from the momentum equations and the pressure field is determined by solving a pressure or pressure correction equation which is obtained by manipulating continuity and momentum equations (Fluent Inc. 2006).

More specifically the pressure-based segregated algorithm was used instead of the coupled algorithm. The coupled solver would improve convergence of the solution but at the same time, the memory requirement would double because all the continuity equations need to be stored in memory when solving for the velocity and pressure fields. The diagram below explains the process visually.
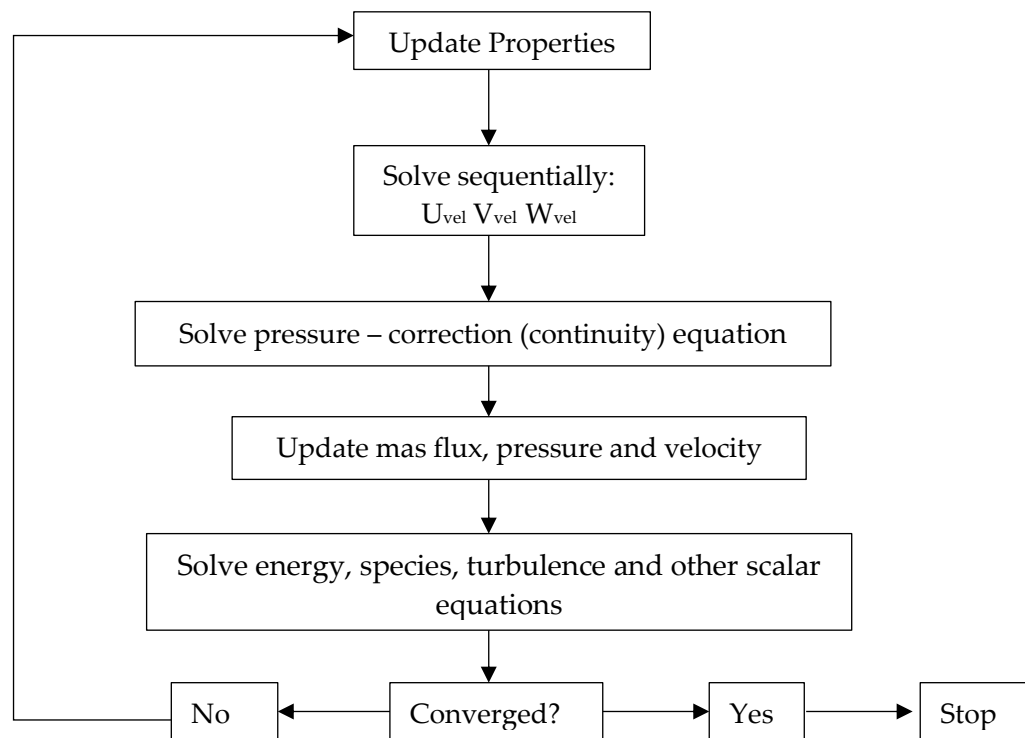
Figure 16. Overview of Pressure-Based Solution Algorithm Used in The Simulations
(Fluent Inc. 2006)

## 4.5. Residual analysis

A successful CFD simulation needs to demonstrate a level of convergence. It was chosen to have a level of 20 iterations for each time step to allow proper convergence. Residual plots are useful to detect proper problems.  In Figure 17 below show the number of iterations and the level of error relating to each part of the numerical model while it is being solved.
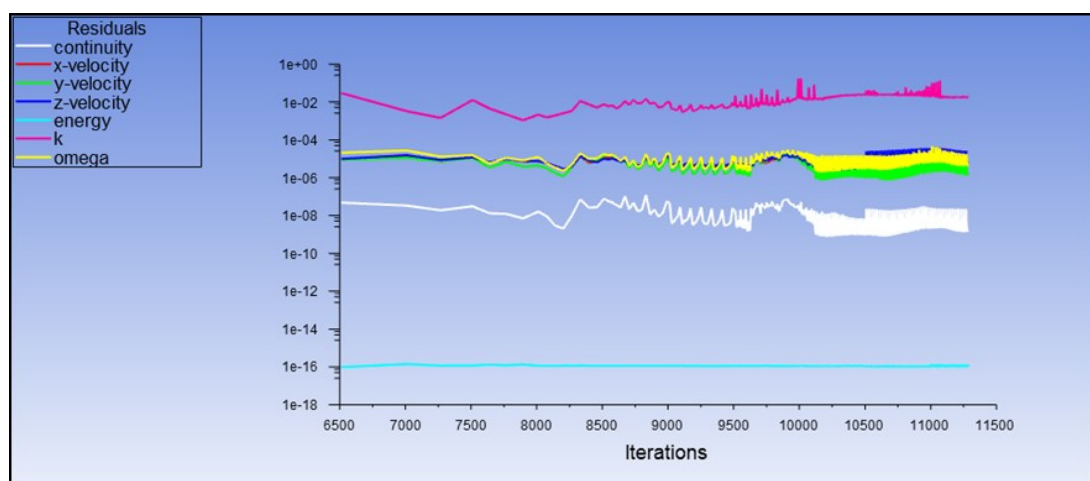


Figure 17. Residual Plot from Fluent Model

In the Residual plot above the levels for convergence for continuity in Ansys fluent is $1e^{-06}$ based on the Ansys literature. As the level of residuals in figure 17 get down to between $1e^{-08}$ to $1e^{-10}$ it is clear to say that the solution has converged in terms of continuity. In relation to the velocities, energy and the omega residuals they are all staying throughout the majority of the iterations at $1e^{-5}$. Only the K residual stays higher at $1e^{-02}$.

# Chapter 5 Case Study

## 5.3. Overview

The objective of using the scenario set out in the paper by Therond, et al. is to have a real-world pressure scenario and realistic cement base for the numerical model. The data displayed in Figure 18 is from the Gulf of Mexico and shows with measured depth the equivalent mud weight in pounds per gallon for the pore pressure in blue, the sandstone fracture pressure in red, the shale fracture pressure in green and the cementing equivalent circulating density in grey. The overburden pressure is on the right in black.
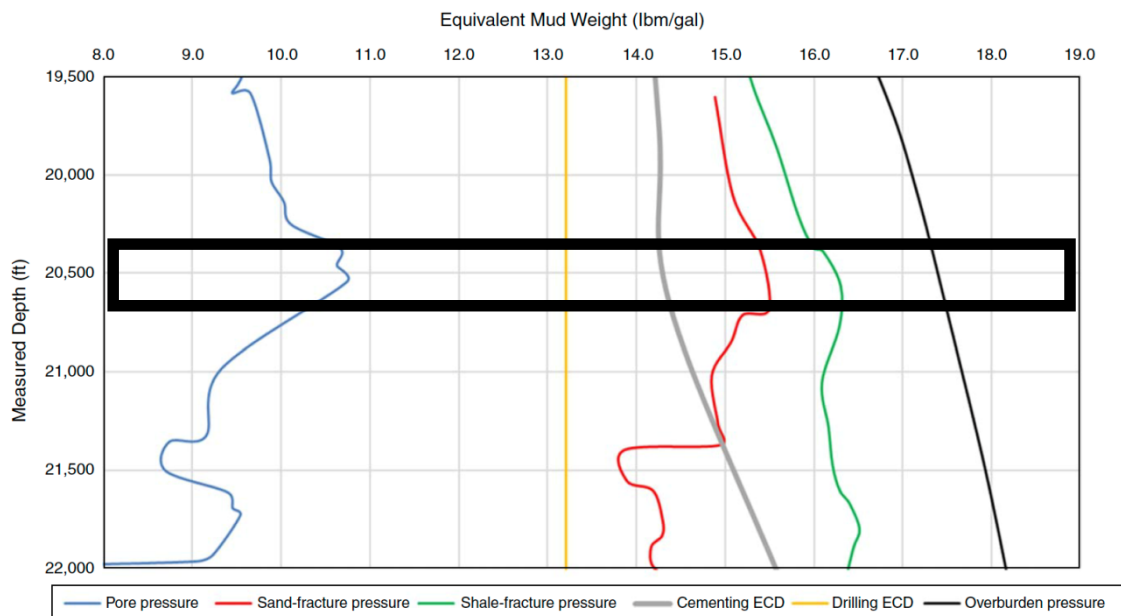


Figure 18. Pressure Regime Used in the 3 Scenarios at 20,500 Feet, highlighted by the Black Box (Therond, et al. 2018)

The scenarios that will be studied based on the baseline information provided by the Therond paper will be focusing on the different flow rates of the cement in three separate scenarios which each have different cement properties, varying in density and viscosity. These then will be tested with 3 different rock formations, a sandstone, limestone and a dolomite.

# 5.4.  Data Description

## 5.4.1. Assumptions

The constants that are used in the simulations are displayed in the table below, they are based on the case study outlined above. These include the depth so that the hydrostatic pressure can be calculated and also the temperature using the gradient typical for the environment stated in the case study of the Gulf of Mexico. Then also the calculated maximum and minimum effective stresses which consider the formation pore pressure. Also, the overburden stress which is the cumulative stress from the rock above the scenario depth.

| *Parameter* | *Field Unit* | *SI Unit* |
|---|---|---|
| Depth | 20,500 ft | 6,248.4 m |
| Hydrostatic Pressure | 0.655 psi/ft (12 ppg mud) 13,431.6 psi | 926 bar |
| Formation Permeability | 200 md | - |
| Formation Temperature | 460 K | 187 $^0$c |
| Porosity | 15% | - |
| Pore Pressure | 11,459.4 psi | 790 bar |
| Formation Density | 128.28 lb/ft$^3$ | 2055 kg/m$^3$ |
| Formation          Fracture Pressure | 16,416.4 psi | 1132 bar |
| Overburden Stress | 18,441.5 psi | 1272 bar |
| Minimum Stress | 11,479.7 psi | 791.5 bar |
| Maximum Stress | 12,183.2 psi | 840 bar |

Table 3. Simulation Model Constant Parameters

## 5.4.2. Simulation Setup

With the model created to contain the case study scenarios The general setup window was used to start with selecting the pressure based, transient solution. Then also the absolute velocity formulation and gravitational acceleration in the Y plan or vertically.

The next step is to select the type of models to use.  Just to recap the multiphase model using the volume of fluid was selected using 2 phases, the drilling fluid and the cement. The energy equation was also turned on along with the viscous fluid model and as the fluids are non-Newtonian the K-omega standard viscous model was used. The setup parameters were changed for each scenario. The courant number for all simulations was set to 0.25, as this gave a good basis for the time steps and helped to provide a good level of accuracy.

## 5.4.3. Simulation Material Properties

Below is the material parameters described for the designed scenarios. To begin with the scenario properties for the first scenario are described and then under that the differences to the 2nd and 3rd scenarios are also laid out. The material properties given are those that are needed for the simulations to function.

The cement parameters are as follows:

- Density 1965.15 Kg/m³
- Specific heat 1006.43 j/kg-k
- Thermal Conductivity 0.0242 w/m-k
- Viscosity, using the Herschel Bulkly fluid type which best suits cement.
  - Consistency Index (k) 2.42 kg-s^n-2/m
  - Power Law Index (n) 0.552
  - Yield stress threshold (pascal) 3.99e+07
  - Critical shear rate (1/s) 0.001
- Molecular weight 28.966 kg/kmol
- Reference temperature 298.15 k

For the drilling fluid the parameters are as follows:

- Density 1509.81 Kg/m³
- Specific heat 1006.43
- Thermal Conductivity 0.0242 w/m-k
- Viscosity, using the Power Law fluid type which suits the drilling fluid
  - Reference Viscosity 0.038 kg/m-s
  - Reference temperature 293k
  - Temperature Exponent 0.666

The Sandstone which surrounds the annulus has the following parameters:

- Density 2055kg/m³
- Specific heat 871 j/kg-k
- Thermal conductivity 202.4 w/m-k

The Limestone which surrounds the annulus in the additional simulations has the following density:

- 2800kg/m³

The dolomite that is also used in additional simulations has the following density

- 2840 kg/m³

The rocks physical properties will be covered in more detail in the following sections. The casing has some simple parameters as the boundary is a fixed wall and is stationary:

- Density 8030Kgm3
- Specific Heat 502.48 j/kg-k
- Thermal Conductivity 16.27 w/m-k

The only variations for the other two scenarios are the density and viscosity which are changed as stated in the variables section to 130 cp for the viscosity and 1737.48kg/m3 for the density in scenario 2 and 1467.87 kg/m3 for the density and 105cp for the viscosity in scenario 3.

## 5.4.4. Boundary Conditions

The inlet becomes a velocity inlet with the magnitude range of 0.75 m/s which is the same flow rate as 0.5bbl/min which is the typical cementing flow rate, this then was staged up and down for each of the scenario 's from 0.01m/s to 6m/s which is 4 bbl./min.

The temperature in the entire model in all scenarios is set to 460k or 187 degrees Celsius. The interior of the fluid zone uses the volume of fluid method taken from the model's section. Then the outlet or pressure outlet has also a temperature of 460k. The gauge pressure taken at this point is the difference between the hydrostatic pressure of the drilling fluid which is 13431.6psi, this is subtracted from the cement equivalent circulating density of 17,482psi leaving a gauge pressure of 4050psi. For the second two scenarios, their gauge pressures were 2025.4psi for scenario 2 and 106.6psi for scenario 3, the two walls, the sandstone and the casing wall have a no slip surface and are both stationary. The casing has a roughness of 0.0002m and a roughness constant of 0.5. The sandstone has a roughness of 0.009m, the Limestone roughness was, and the dolomite roughness was and a roughness constant of 0.5.

## 5.4.5. Transient Structural Setup

The transient settings vary as there is no flow taking place. This model takes the resultant pressure from the fluent model and uses this to simulate the interaction between the contacts.

- Analysis settings
    - 6-time steps each with 0.1111 seconds making up the same time as the fluent model of 0.6666 seconds.
    - The model uses standard earth gravity
    - The hydrostatic pressure of the drilling fluid is 97.46Mpa
    - The minimum horizontal stress was 79.01 Mpa
    - The maximum horizontal stress was 84.0 Mpa
    - Around the sandstone there is a fixed support to stop the expansion of the model
    - The imported load taken from the fluent model is used on the outer circumference of the annulus as this is the area of interest.
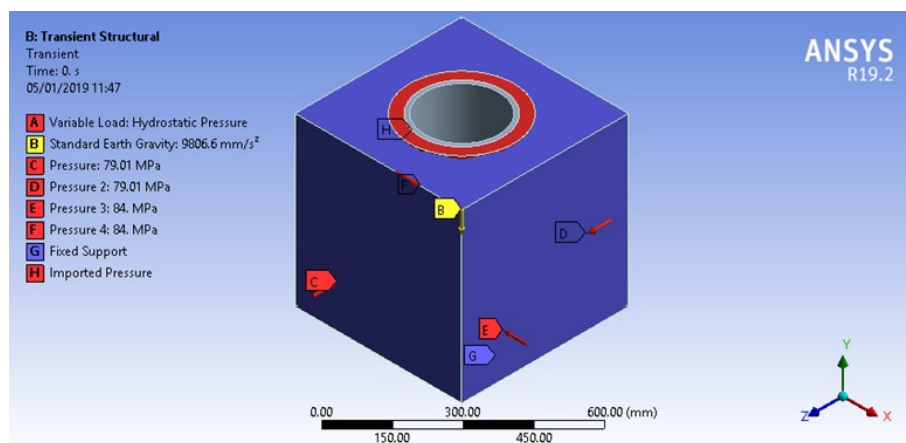


Figure 19. Pressure Regime for Transient Structural Model

The pressure regime displayed in Figure 19 is based on the case study data which is described in the following section. The pressure scenario has from above the hydrostatic pressure (A), based on the drilling fluid being present from the case study depth 13,431.6psi) until the surface. The standard earth gravity represented by the yellow B is acting on the whole geometry. The stresses or pressures C and D are the minimal principal horizontal stresses which are 79.01mpa, calculated by using this equation:

$$Shmin \ = \ (\vartheta/1 - \vartheta) \ (Sv - PP) \ + \ PP \tag{7}$$

(Economides 1992)

Where,

- $\vartheta$ is poisons ratio
- PP is pore pressure
- $Sv$ is overburden stress

Then the pressures E and F are the maximum principal stresses, 84mpa. Calculated by using the following equation:

$$SHmax \ = \ \left(\frac{\vartheta}{1} - \vartheta\right)(Sv - PP) + \ PP + STect \tag{8}$$

(Economides 1992)

Where,

- $STect$ is tectonic stress

In the model the G represents the purple boundary outside of the rock structures this holds the model in place so that the internal pressures don't affect the entire geometry. The final pressure or stress in this model is H which is the imported stress from the fluent model. This acts in the annulus fluid zone against the formation/fluid interface.

## 5.5. Studied Scenarios

The Variables described in Table 4 are related to each scenario. It displays the cement density of each scenario and the varying viscosity. Then the various velocities used in the simulations are displayed, starting at 0.01 m/s up until 6 m/s. The deformation, volumetric change and associated stresses will be calculated using the numerical model in Ansys Fluent and Transient Structural models. The minimum velocity chosen was to show the simulation operating with almost zero equivalent circulating density and therefore just the hydrostatic pressure operating. Later the variation in velocities will be compared against the variation in stresses and deformation.

| Variable | Scenario 1 | Scenario 2 | Scenario 3 |
|---|---|---|---|
| Cement Density | 16.4 ppg (1965.15 kg/m3) | 14.5ppg (1737.48 kg/m3) | 12.5 ppg (1467.87 kg/m3) |
| Cement Viscosity | 155 cp | 130cp | 105 cp |
| Cement Velocity | 0.01 m/s<br>0.375m/s<br>0.75 m/s<br>1.0m/s<br>1.25 m/s<br>3 m/s<br>6 m/s | 0,033 ft/sec<br>1.230 ft/sec<br>2.460 ft/sec<br>3.280 ft/sec<br>4.101 ft/sec<br>9.842 ft/sec<br>19.685 ft/sec | |
| Cement Displacement Rate | 0.001 m³/hr<br>0.04 m³/hr<br>0.08 m³/hr<br>0.1 m³/hr<br>0.13 m³/hr<br>0.32 m³/hr<br>0.64 m³/hr | 0.006 bbl/hr<br>0.25 bbl/hr<br>0.5 bbl/hr<br>0.67 bbl/hr<br>0.83 bbl/hr<br>2 bbl/hr<br>4 bbl/hr | |

Table 4. Simulation Model Variable Parameters

## 5.5.1. Formation Variations

The different formations used have different properties. Table 5 describes the different properties of the materials used in the transient structural mechanical model. The differences between the properties can be quite vast due to the diverse uses of each material in well design and then also the naturally occurring formations which have properties born out of their geological environment of deposition.

Each rock will be tested in turn against each scenario at both a low velocity cement in each scenario at 0.01m/s and the middle case or base case 0.75m/s. Then the subsequent levels of deformation and volumetric change along with the stresses caused will be recorded.

| | Density (kgm3) | Youngs modulus (Mpa) | Poisson's Ratio | Bulk Modulus (Mpa) | Shear Modulus (Mpa) |
|---|---|---|---|---|---|
| Sandstone | 2055 | 34007 | 0.23 | 21300 | 13780 |
| Limestone | 2800 | 37845 | 0.31 | 32800 | 14470 |
| Dolomite | 2870 | 58589 | 0.28 | 44800 | 22850 |
| Casing | 8030 | 200000 | 0.3 | 166670 | 76923 |
| Cement | 1890/1737.48/1467.87 | 30000 | 0.24 | 19231 | 12097 |

Table 5. Material Properties for the Transient Structural Mechanical Model

## 5.5.2. Solution Method

To solve the fluent simulation there are some methods that have to be selected, the scheme to solve the model is called simple and for the pressure Presto!, then to solve the momentum a second order equation is used and also for the kinetic energy.

Then using the same gauge pressure as the outlet and the fluid velocity the calculation can be initialised, also at this stage the fluid zone needs to be set to 100% drilling fluid so that the cement can flow inside displacing the drilling fluid. The final step was to set the time step size of 0.005 seconds, with 1334 steps which equals the same amount of time it will take to fill the fluid zone with cement at a rate of 0.75m/s.
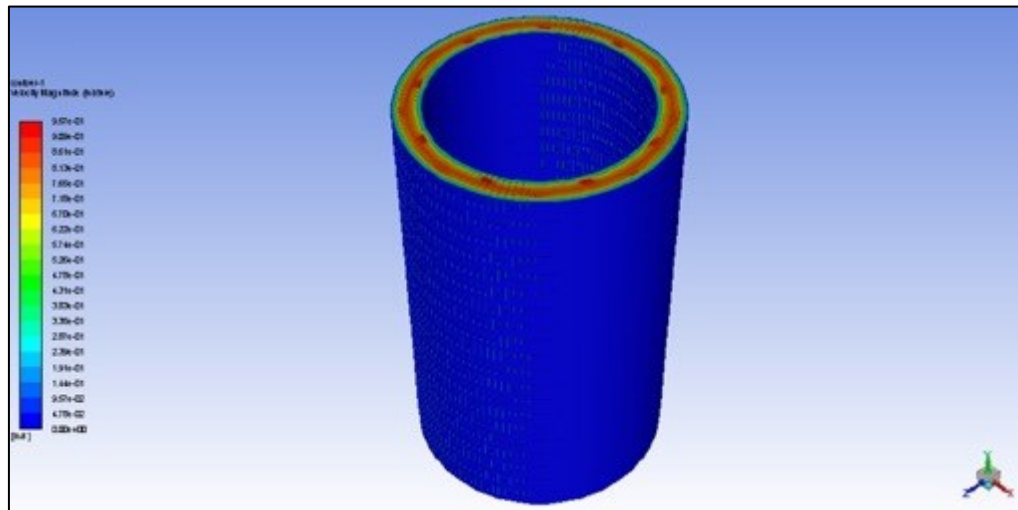


Figure 20. Velocity Distribution in Fluid Zone

Figure 20 shows the velocity distribution and how it is spread in the fluid zone of the annulus. The highest velocity can be seen in the centre on the annulus as a red ring which is away from the walls where the flow velocity is lower. This is a normal flow distribution for fully developed flow.

Then the pressure distribution is displayed in Figure 21 this shows the highest pressures occurring towards the base of the zone, this is where the hydrostatic pressure is at its highest and where the cement flow is first developed overcoming the hydrostatic pressure of the drilling fluid above.
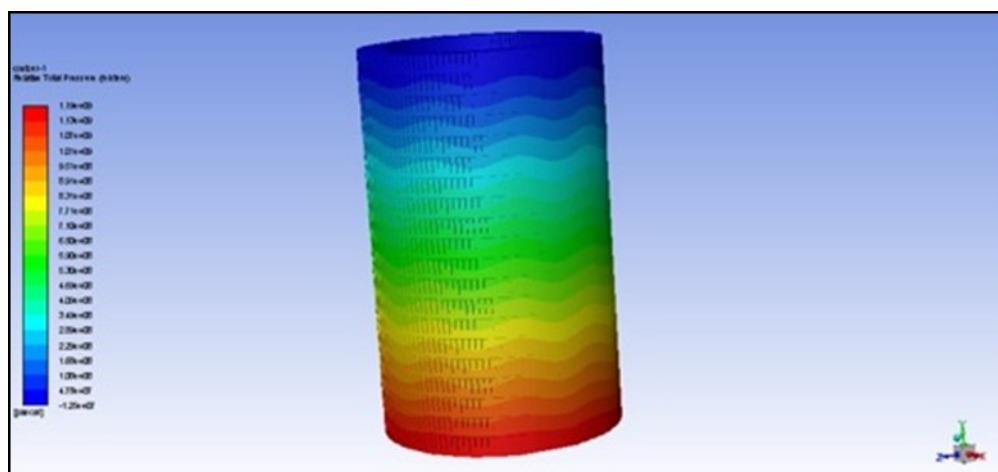


Figure 21. Pressure Distribution in the Fluid Zone at the Final Time Step

# 5.6. Results and Discussion

In order to perform meaningful analysis, it was decided to use a sandstone as the main lithology which was also compared later to two other lithologies, limestone and dolomite. Low velocities were used to mimic a static case or pumps off and varying densities were used to imitate tail and lead cement, this then was simulated at varying velocities in different lithological environments.

## 5.6.1. Velocity Effects on Cement and Rock Deformation

### 5.6.1.1 Radial Deformation

Radial deformation in Ansys is defined as total deformation this is used to obtain displacements from stresses. For total deformation, it gives a square root of the summation of the square of x-direction, y-direction and z-direction. The average radial deformation was chosen. The levels of deformation seen in Figure 22 show that the maximum deformation is similar for each of the scenarios but with Scenario 1 having a marginally greater level of deformation at 1.27mm. Scenario 2 had a maximum of 1.26 and Scenario 3 had also a maximum of 1.26. The average values showed a larger deformation for Scenario 3 at more velocities with a value of 0.41 at 3 velocities, 1.25m/s to 6 m/s. Scenario 2 with slightly less at 2 velocities with 0.41mm and one at 0.406mm when the velocities are at 1.25m/s, 3m/s and 6m/s and Scenario 1 with just 1 velocity with 0.41mm average deformation when at 3m/s.

The levels of deformation are displayed in Figure 22 with scenario 3 showing the fastest acceleration in deformation, scenario 2 second and scenario 1 third.
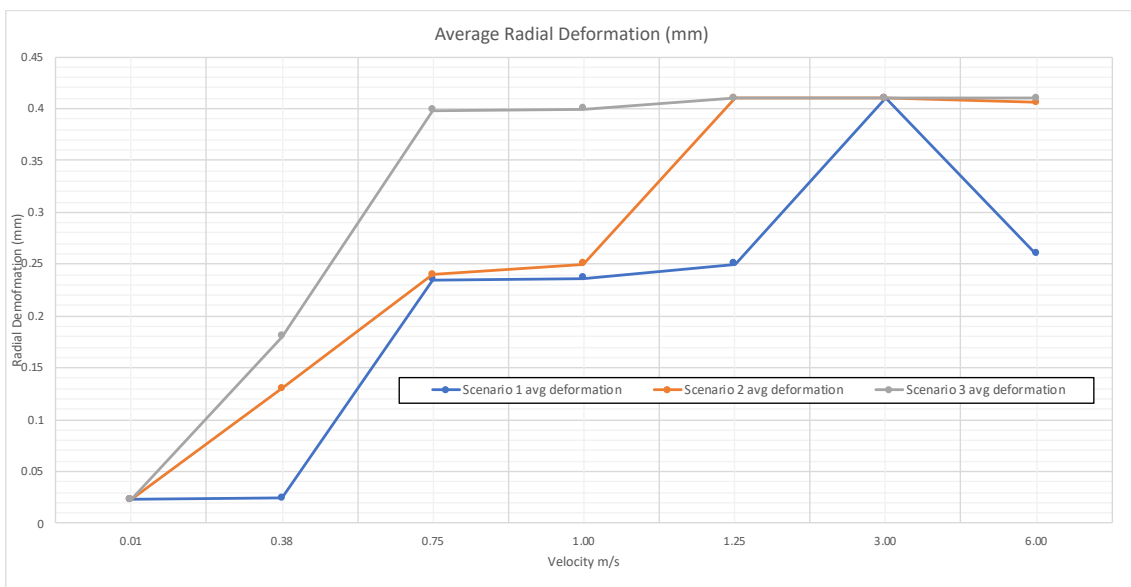


Figure 22. Deformation for Each Scenario at the Different Velocities

The average radial deformation for Scenario 1 shows that after 0.375m/s begins to cause deformation which then stabilises at 0.75m/s and then increases again at 3m/s with a maximum value of 0.41mm then returning back down to 0.236 mm at 6m/s. Scenario 2 follows a similar pattern showing linear deformation, to begin with up to

0.75m/s and the stabilises for one velocity before peaking and stabilising at 0.41mm. Scenario 3 has a slightly different behaviour, immediately causing deformation of 0.41mm at 0.75m/s which it then stabilises at for the subsequent velocity models.

## 5.6.1.2 Volumetric Change

Figures 23 to 25 show in visual form the amount of volumetric increase for the individual scenarios at the velocities set. The levels of volumetric change increase with each increasing velocity. In Scenario 1 as seen in Figure 23 the volume increase starts at $0.003cm^3$ with the velocity 0.01m/s but increases to $0.90cm^3$ by 1.25m/s and stays at this level.
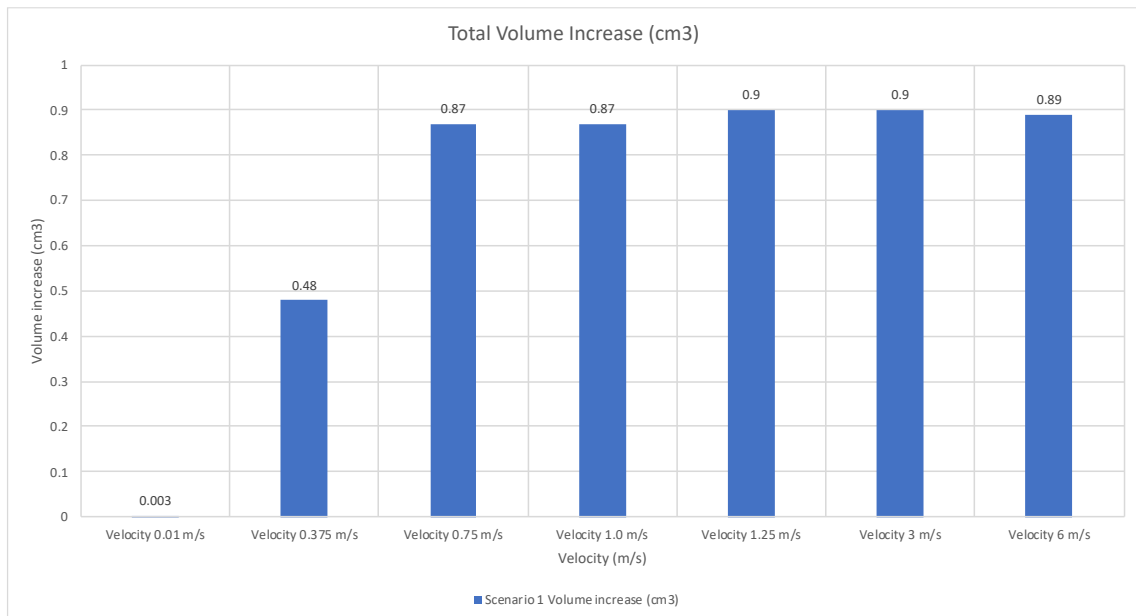


Figure 23. Graph Displaying the Volumetric Changes in Scenario 1 at the Prescribed Velocities

For Scenario 2, in Figure 24, the volumetric increase starts at 0 for the velocity 0.01m/s and then goes up to $0.89cm^3$ by 1.0 m/s but then stabilises at this level for the subsequent velocities.
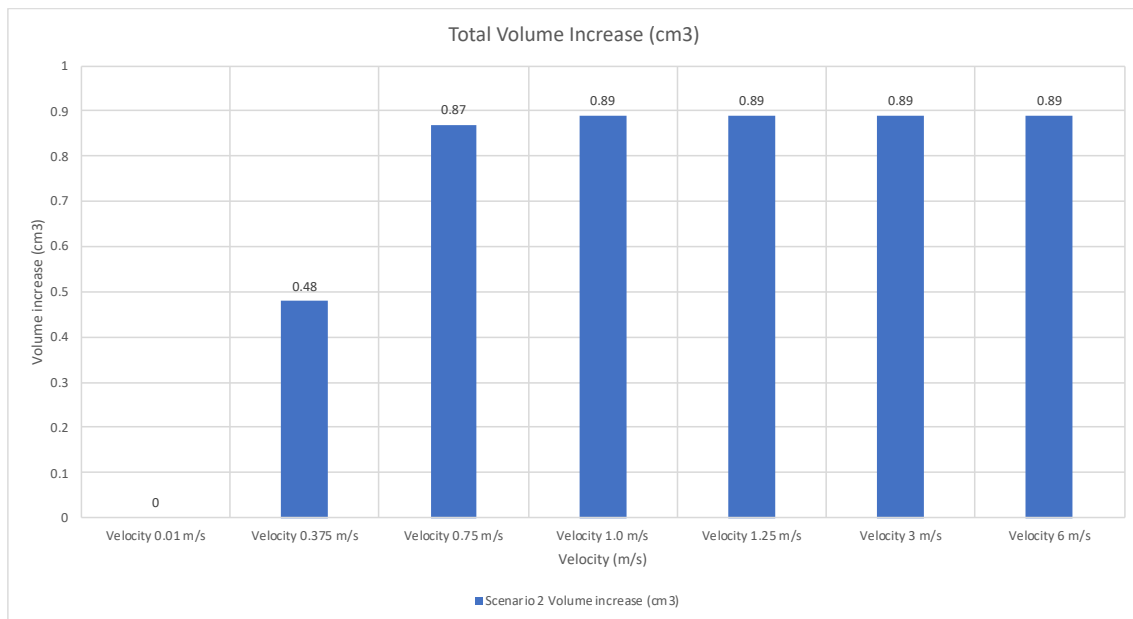
Figure 24, Graph Displaying the Volumetric Changes in Scenario 2 at the Prescribed Velocities

In Figure 25, Scenario 3 follows a similar behaviour, starting at 0 cm³ volumetric change at 0.01m/s and then increases to 0.89cm³ at 1.0m/s.
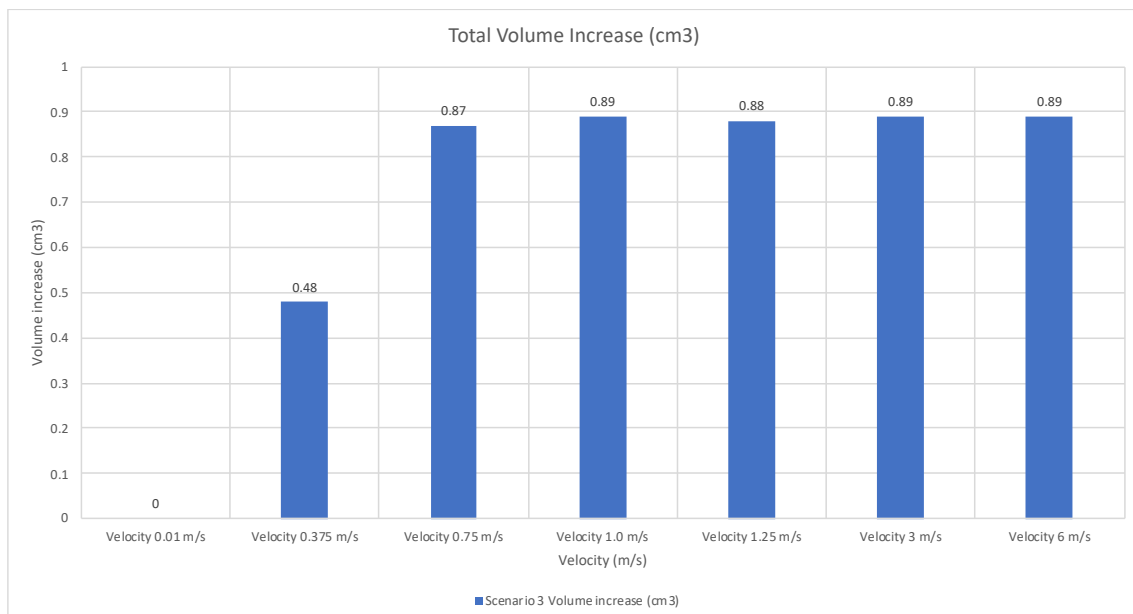


Figure 25, Graph Displaying the Volumetric Changes in Scenario 3 at the Prescribed Velocities

The volume increase shown at 0.01m/s was 0.003cm3 for cement scenario 1 and for the other two scenarios was zero. At 0.375m/s the volumetric change was 0.48cm3 for all three scenarios. At 0.75m/s the volumetric change was up to 0.87cm3 for all types of cement tested. With the velocity at 1m/s the volumetric change stayed at 0.87cm3 but the other two scenarios had a slightly larger increase to 0.89cm3 for scenario two and three. The volumetric changes levelled out for the subsequent velocity increases with minor variations between the types of cement with cement scenario one reaching the

highest level of volumetric change at 0.9cm$^3$. By 6m/s the volumetric increases for all three scenarios stabilised at 0.89cm$^3$.

As can be seen in the 3 figures above when the cement is under a velocity there is a very small volumetric increase and then when the cement stops being pumped this will then return to the volumetric increase of the minimum velocity which is incredibly small this then will affect the level of deformation that occurs.
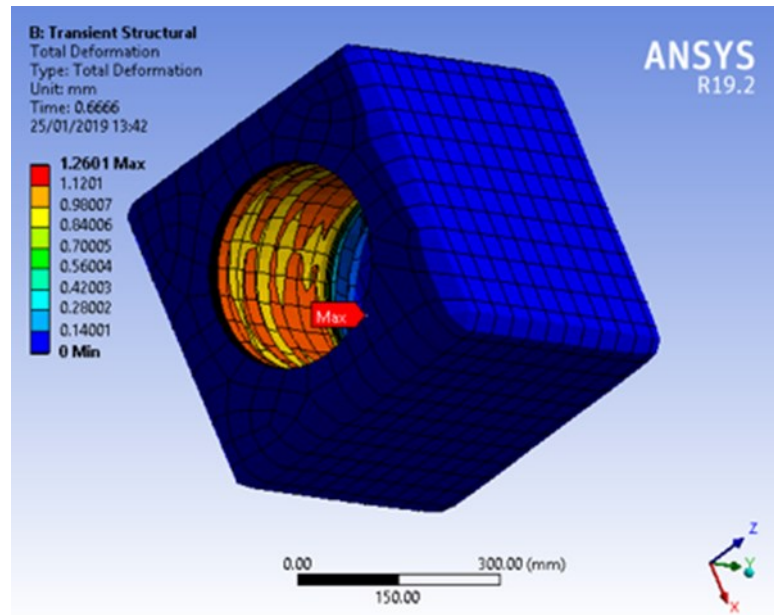


Figure 26. Visible Deformation on the Sandstone Body

In the visualization above (Figure 26), the deformation can be seen from the simulation of the cement scenario 2 with the velocity of 1.0m/s at the timestep 0.666 seconds.
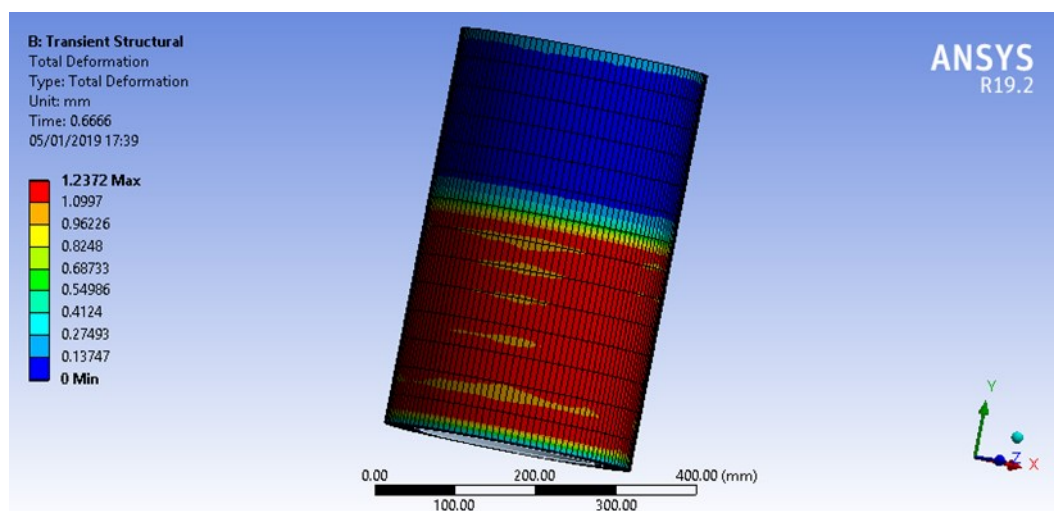


Figure 27. Annulus deformation which is transferred onto the sandstone

Figure 27 shows cement scenario 1 at 0.75m/s which equates to 0.5bbl/min. The figure shows the deformation around the annulus and the variation of its distribution on the fluid/formation interface.

Using the data obtained a formula was conceived using regression to predict the volumetric change as a function of density, viscosity and velocity. An analytical equation was used to estimate the volumetric change. The following equation was set up to be used for sandstone but similar steps can be followed to determine the equations for other rock types.

$$Volumetric\ Change = \tag{9}$$

$$0.67528 + 0.032026 * Velocity + 0.01667 * Density - 0.00127 * Viscosity$$

## 5.6.1.3 Stress Analysis

The stresses used as a part of the analysis are the Equivalent stress (also called von Mises stress) which is often used in design work because it allows any arbitrary three-dimensional stress state to be represented as a single positive stress value. The other stresses such as the maximum and minimum principal stresses, these are the stresses working out from an infinitesimally small volume and are normalised. The maximum shear stress is the maximum stress on the Mohr circle as a combination of the 3 principal stresses and is the stress acting on the rock from the cement.
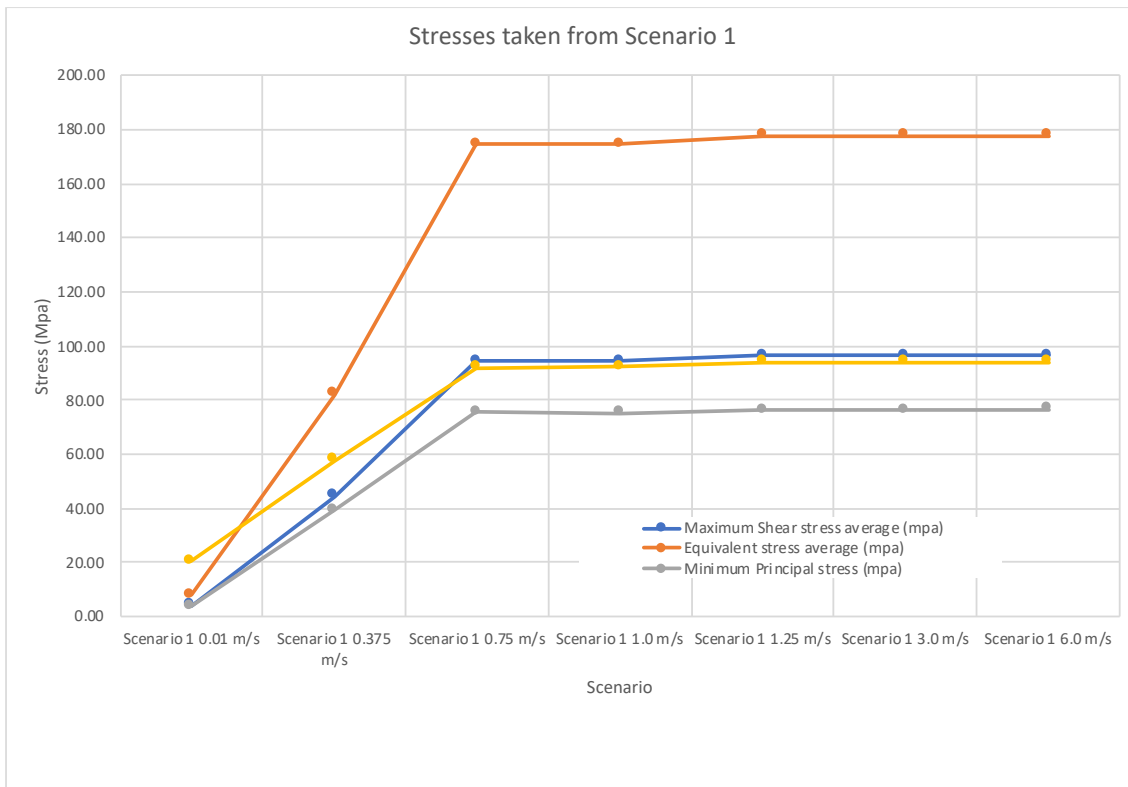


Figure 28. Stresses Given in Scenario 1 at Varying Velocities

In Figure 28 the stresses are given from cement scenario 1 with each velocity compared. The stresses react in a similar way to the volumetric changes. At low velocities the stresses are minimal, with the Maximum principal stress marginally higher than the other stresses. At 0.01m/s the stresses are very low, they then take a step up at 0.375m/s. As the velocities increase up to 0.75m/s the stresses also increase. The stresses then level out and remain constant as the velocities increase. This means that after a certain velocity level the stress levels are constant once the flow is fully developed. The maximum shear stress reaches nearly 100Mpa at 0.75m/s.
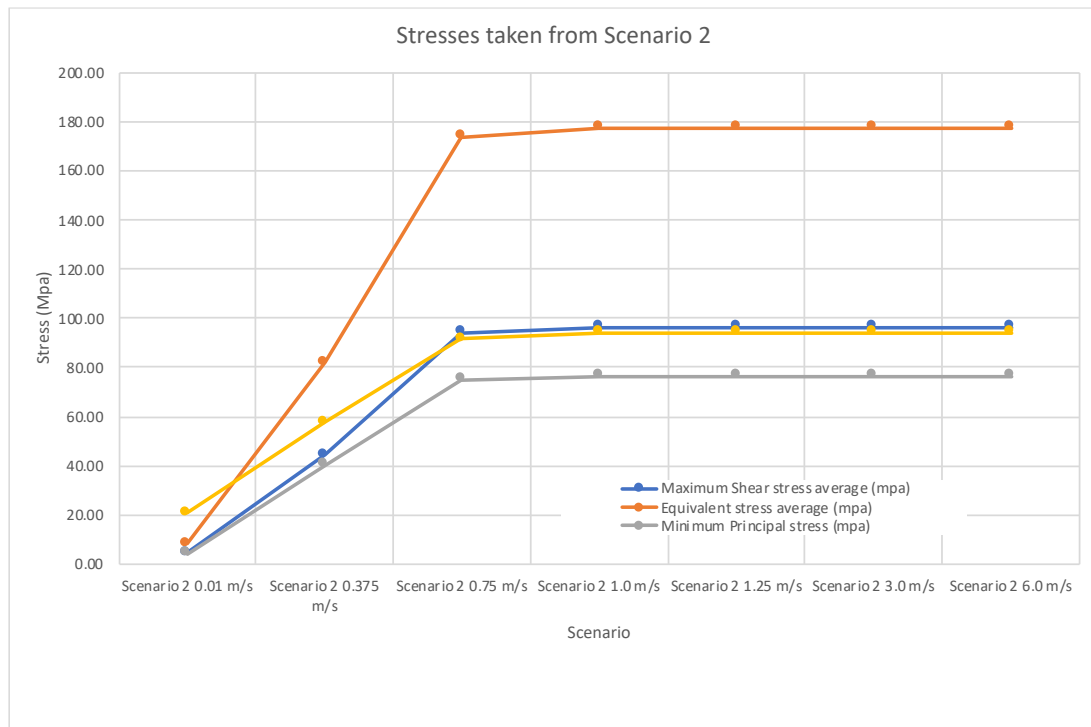


Figure 29, Stresses Given in Scenario 2 at Varying Velocities

In Figure 29 the stresses are given from cement scenario 2 and also shows the velocities applied. The stresses react in a similar way to the previous scenarios and the volumetric changes. At 0.01m/s the stresses are very low, they then take a step up at 0.375m/s., with the maximum stress being the equivalent stress at just above 80Mpa. As the velocities increase up to 0.75m/s the stresses also increase. The stresses then level out and remain constant as the velocities increase.
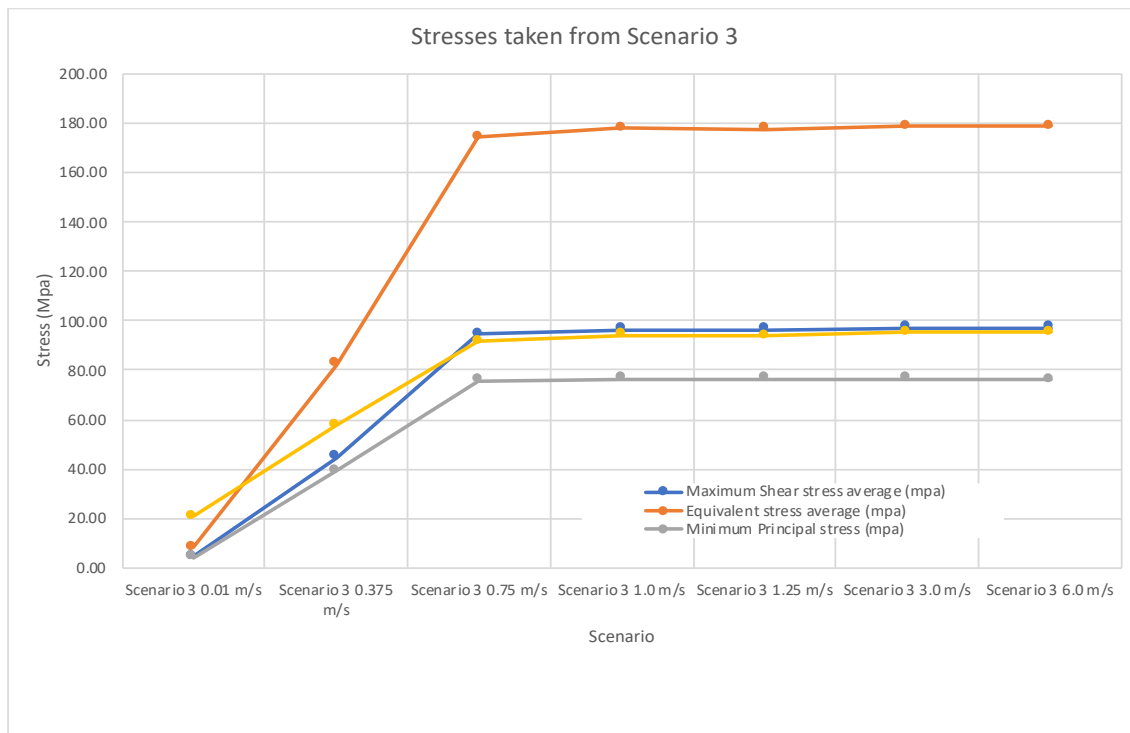
Figure 30. Stresses Given in Scenario 3 at Varying Velocities

In Figure 30 the stresses are given from cement scenario 3 and also with each velocity the results are compared. The stresses react in a same way as Scenario 1 and 2. At low velocities the stresses are minimal. Starting at 0.01m/s the stresses are very low, they then increase up to when the velocity is at 0.75m/s. Then the stresses peak and then level out and remain constant as the velocities increase.

## 5.6.2. Effects of Formation Type on Cement and Rock Deformation

### 5.6.2.1. Stress Analysis

The stress exerted is on the rock from the cement slurry being pumped. In Figure 31, 32 and 33 below show a comparison between different rock types and the levels of stress at 0.75m/s for each cement scenario. Also, the results for the simulations run with a velocity of 0.01m/s can be seen in the Appendix in table 9. The dolomite rock encountered the most stress in each scenario and also showed the lowest amount of volumetric change, this shows the dolomite can withstand a higher amount of stress before deforming compared to the limestone and sandstone.

Figure 31 also shows that the equivalent stress is at its highest when combined with the sandstone. The minimum and maximum principal stresses were at their lowest with the sandstone but at their highest with the dolomite. The equivalent stress was at its highest for the sandstone.
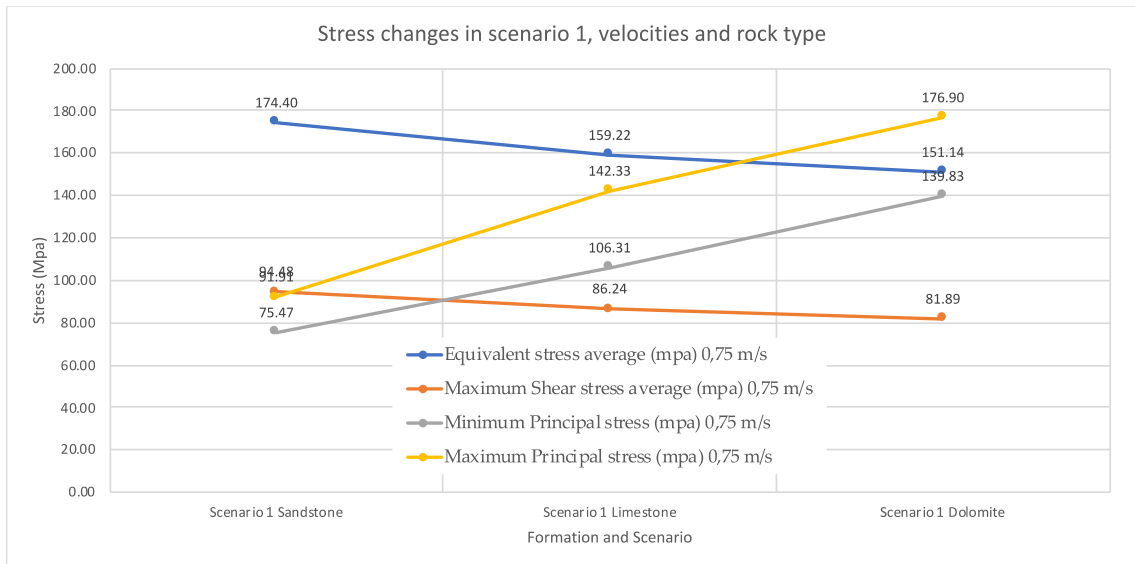
Figure 31. Stress Changes for Scenario 1 at 0.75m/S

Figure 32 below also shows that the equivalent stress is at its highest when combined with the sandstone. The minimum and maximum principal stresses were at their lowest with the sandstone and at their highest with the dolomite. The equivalent stress was at its highest for the sandstone.
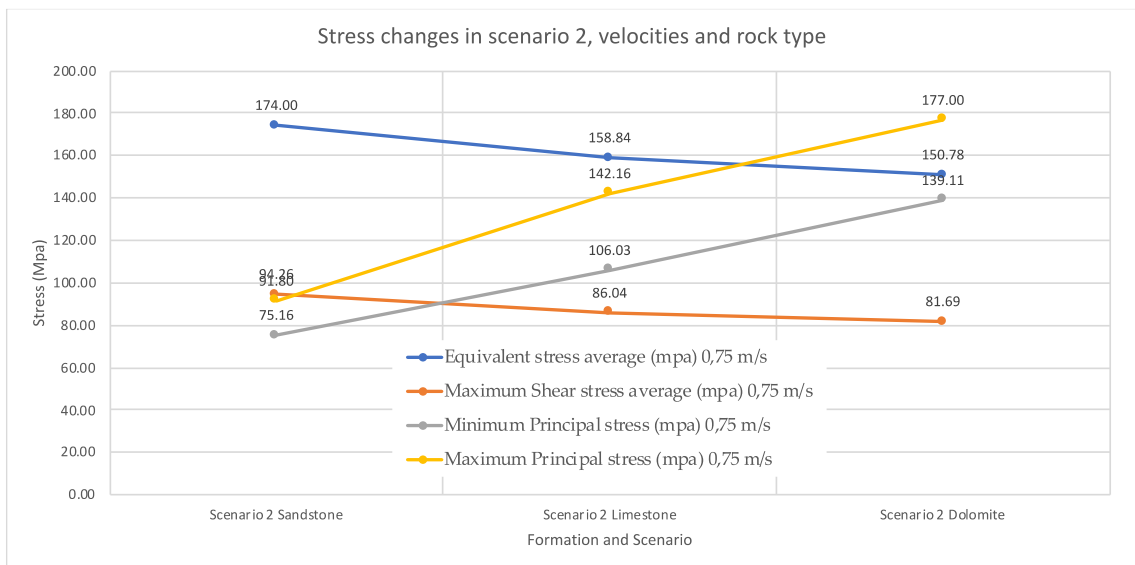


Figure 32. Stress Changes for Scenario 2 at 0.75m/S

In Figure 33 the same pattern is followed for the stresses with each rock type. Maximum and minimum principle stresses increasing from sandstone, to limestone and then with the highest in the dolomite formation environment.
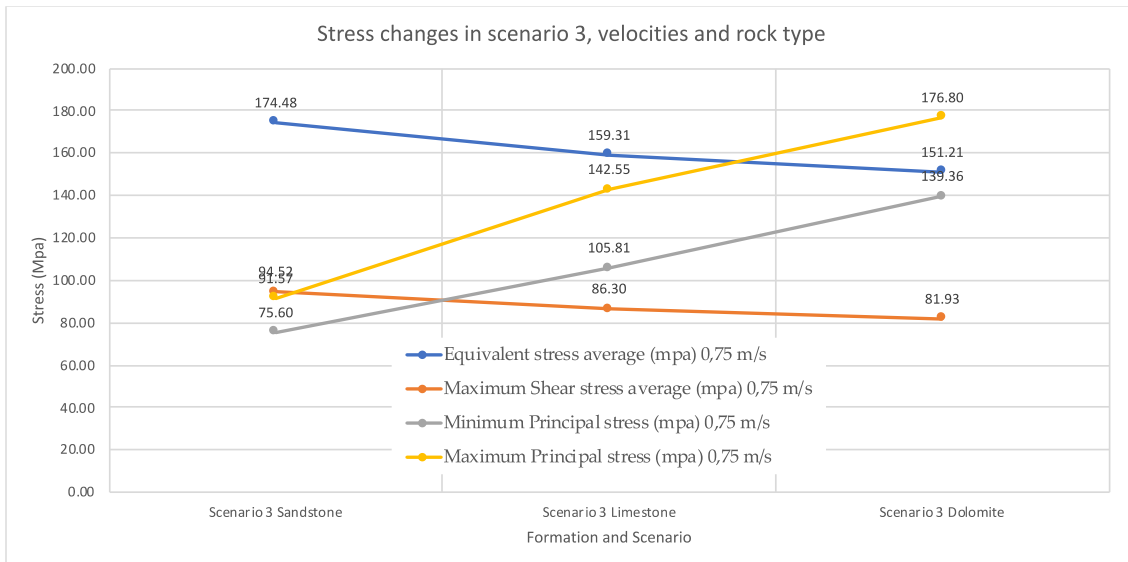
Figure 33. Stress Changes for Scenario 3 at 0.75m/S
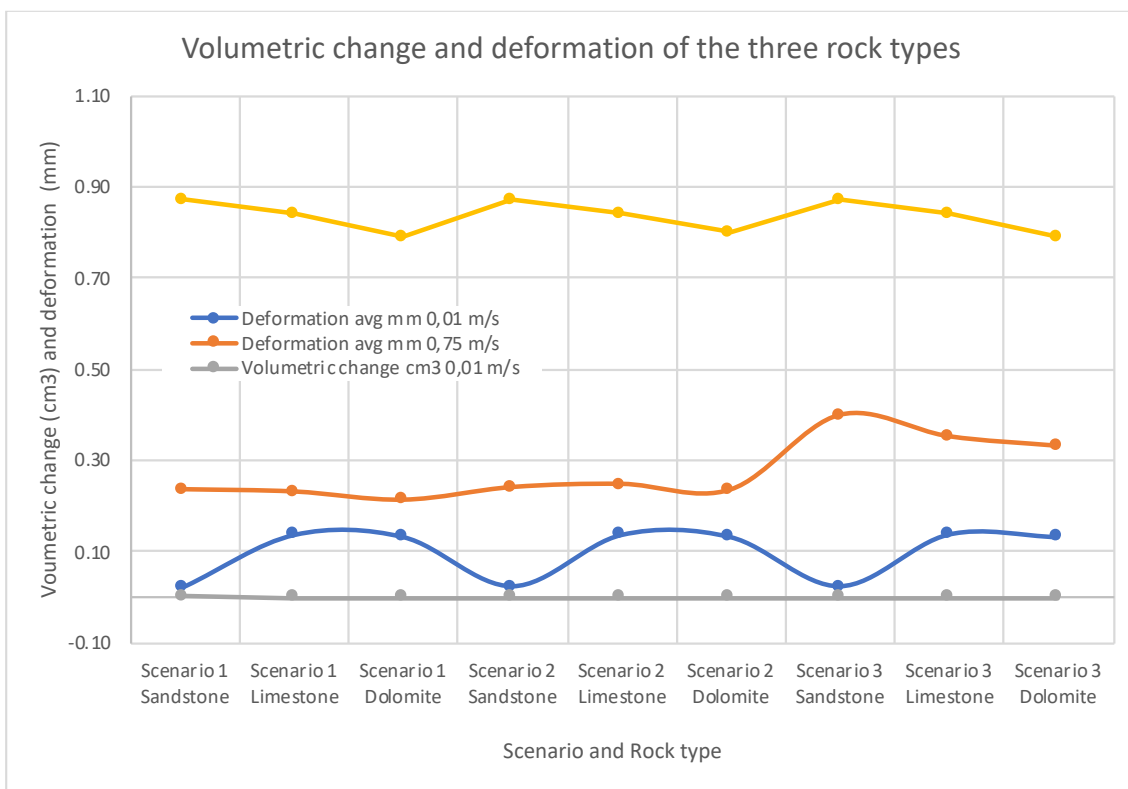
## 5.6.2.2. Volumetric Changes and Deformation



Figure 34. Volumetric Change and Deformation for the Three Rock Types

Above in Figure 34 is the visual form of the deformation and volumetric changes at 0.01m/s and 0.75m/s. The differences can be seen with different rock types within the same cement scenarios. In particular focus is scenario 3 in

Figure 34 at 0.75m/s the sandstone shows the highest levels of deformation and volumetric change in comparison with the other two rocks in this scenario. For the other two scenarios the level of volumetric change is relatively constant.

## 5.7. Case Study Conclusion

Gaining a comprehensive understanding of cement deformation is imperative to overall wellbore integrity. This understanding with the help of these simulations has the potential to help and improve cement integrity. After the simulations and analysis of all the cement scenarios and with each velocity a clear pattern emerges that above 0.75m/s the deformation and volumetric changes stabilize. The major differences occur between 0.01m/s and 0.75m/s.

Cement scenario 1 with a density of 1965.15 Kg/m3 and a viscosity of 155cp doesn't deform as much or as a faster rate in the sandstone formation as the other two scenarios but the volumetric changes are very similar for all scenarios. At 0.01m/s the stresses are very low, they then take a step up at 0.375m/s. As the velocities increase up to 0.75m/s the stresses also increase. The stresses then level out and remain constant as the velocities increase. This means that after a certain velocity level the stress levels are constant once the flow is fully developed. The maximum shear stress reaches nearly 100Mpa at 0.75m/s.

In Scenario 2 the stresses react in almost exactly the same way as Scenario 1.
At 0.01m/s the stresses are very low, they then take a step up at 0.375m/s., with the maximum stress being the equivalent stress at just above 80Mpa. The stresses then level out at 0.75m/s and remain constant as the velocities increase. Scenario 3 reacts in the same way as Scenario 1 and 2. At low velocities the stresses are minimal. Starting at 0.01m/s the stresses are very low, they then increase up to when the velocity is at 0.75m/s. Then the stresses peak and then level out and remain constant as the velocities increase.

Overall the cements in each scenario reacted in roughly the same way as each other providing similar amounts of deformation and volumetric changes.

For the different formations Sandstone had the highest level of volumetric change and deformation. In particular focus at 0.75m/s the sandstone shows the highest levels of deformation and volumetric change in comparison with the other two rocks. For the other two scenarios the level of volumetric change is relatively constant. Limestone was right down the middle in terms of deformation and volumetric changes. Dolomite had a smaller volumetric change than the other rock types.
So, in conclusion when analysing the different rock types, the dolomite has a smaller volumetric change to the other 2 rock types. So, the rock which changes volumetrically by the largest amount is the sandstone.

The ability to detect the flow properties and the pressures and stresses related to this using Ansys can be accurate but there was a limitation with the computational power and therefore the meshing size available. When designing the cement, the formation should be considered when choosing the type of cement and its properties, to expect a larger formation deformation with a sandstone as opposed to a limestone or a Dolomite.

# Chapter 6 Conclusion and Recommendations

## 6.1. Conclusion

To gain an understanding of how geomechanics, structural and fluid mechanics are all related to cement integrity, this thesis has brought them together using a CFD software such as Ansys enabled this to be possible.

A state of the art CFD software was used to run the fluid simulation which ran in tandem with the transient structural mechanical simulation. The software was set up using the parameters from the paper by Therond et al. This created the base for the numerical model. In that paper it states that any likelihood of losses during cement operations was low. Which would lead to thinking that that also there would be a limit to the amount of deformation occurring at the same time and although this paper didn't consider the ballooning formation or the possible volumetric changes that could take place, the outcome of no substantial loss events can also lead to thinking that the formation deformation during this operation would be minimal too.

After the case study and analysis, the total amount of radial deformation for the 0.5m model had a maximum of $0.9cm^3$. When this is extrapolated out to a section of 200m measured depth the amount would be $360cm^3$ or $0.00036m^3$ of additional volume. If for example this section was 1000m as in last several years, the lengths and complexities of wells being drilled has been increasing year on year the amount of volumetric change would equate to $0.0018m^3$.

This very small change in volume over a relatively moderate section length would signify that well integrity issues probably wouldn't become a problem if cementing and cement integrity isn't properly catered for. This small volume can be accounted for with existing amounts of cement or a small amount of extra volumes of cement or by changing the cements properties to reduce the level of deformation.

## 6.2. Recommendations

Fluid dynamics and structural mechanics and its research is a wide and complex field. This thesis was intended to gain an initial understanding of cement and formation behaviour.

This thesis study was limited by a couple of factors, one major factor was the limitation of computational hardware for the simulation runs. Fluid dynamics simulations are immensely computational expensive especially if high resolution mesh models and transient simulations are applied.

The simulations for this thesis were done on an ordinary laptop. For future CFD studies it is strongly recommended to either use a dedicated computational fluid dynamics cluster or rent CPU time in the cloud from a supported high-performance computing service provider which is probably more cost effective for occasional CFD studies.

In future work and analysis, the simulation periods could be extended and adapted to show better the level of deformation a long time after the cement ceases pumping, or focusing on another area of the casing string such as the shoe where velocities with larger elements of deceleration and acceleration which can cause different stresses towards the formation surrounding the casing due to the variations in flow.

# Appendix

## A1.1 Ansys Software used

Intro about ANSYS is a commercial software package that can be used for free for academic use.

ANSYS Fluent software contains the broad physical modelling capabilities needed to model flow, turbulence, heat transfer, and reactions for industrial applications—ranging from air flow over an aircraft wing to combustion in a furnace, from bubble columns to oil platforms, from blood flow to semiconductor manufacturing, and from clean room design to wastewater treatment plants. Fluent covers a broad reach, including special models with capabilities to model in-cylinder combustion, aero-acoustics, turbomachinery and multiphase systems.

More information can be found at https://www.ansys.com/products/fluids/ansys-fluent

Using a combination of Ansys fluent and the Transient structural simulation packages the model was developed. The Fluent side was used to calculate the fluid movement properties and subsequent pressures with the results feeding into the transient structural model to calculate the relative deformation of the formation.

# A1.2 Result tables

| Scenario deformation | Velocity 0.01 m/s | Velocity 0.375 m/s | Velocity 0.75 m/s | Velocity 1.0 m/s | Velocity 1.25 m/s | Velocity 3 m/s | Velocity 6 m/s |
|---|---|---|---|---|---|---|---|
| Scenario 1 maximum (mm) | 0.14 | 0.57 | 1.24 | 1.25 | 1.27 | 1.27 | 1.25 |
| Scenario 1 minimum (mm) | 0.014 | 0.014 | 0.14 | 0.14 | 0.14 | 0.14 | 0.14 |
| Scenario 1 avg (mm) | 0.023 | 0.0235 | 0.235 | 0.236 | 0.250 | 0.41 | 0.236 |
| Scenario 2 maximum (mm) | 0.14 | 0.57 | 1.23 | 1.26 | 1.26 | 1.26 | 1.26 |
| Scenario 2 minimum (mm) | 0.014 | 0.014 | 0.13 | 0.14 | 0.14 | 0.14 | 0.14 |
| Scenario 2 avg (mm) | 0.023 | 0.133 | 0.24 | 0.25 | 0.41 | 0.41 | 0.406 |
| Scenario 3 maximum (mm) | 0.14 | 0.57 | 1.22 | 1.26 | 1.25 | 1.26 | 1.26 |
| Scenario 3 minimum (mm) | 0.013 | 0.14 | 0.14 | 0.14 | 0.14 | 0.14 | 0.14 |
| Scenario 3 avg (mm) | 0.023 | 0.187 | 0.398 | 0.40 | 0.41 | 0.41 | 0.41 |

Table 6. Scenario deformation at each simulated velocity

| | Velocity 0.01 m/s | Velocity 0.375 m/s | Velocity 0.75 m/s | Velocity 1.0 m/s | Velocity 1.25 m/s | Velocity 3 m/s | Velocity 6 m/s |
|---|---|---|---|---|---|---|---|
| Scenario 1 Vol increase | 0,003 cm3 | 0,48 cm3 | 0.87 cm3 | 0.87 cm3 | 0.90 cm3 | 0.90 cm3 | 0.89 cm3 |
| Scenario 2 Vol increase | 0 | 0.48 cm3 | 0.87 cm3 | 0.89 cm3 | 0.89 cm3 | 0.89 cm3 | 0.89 cm3 |
| Scenario 3 Vol increase | 0 | 0.48 cm3 | 0.87 cm3 | 0.89 cm3 | 0.88 cm3 | 0.89 cm3 | 0.89 cm3 |

Table 7. Volume increase for each scenario at the related velocity

| Velocity/Scenario | Maximum Shear stress average (mpa) | Equivalent stress average (mpa) | Minimum Principal stress (mpa) | Maximum Principal stress (mpa) |
|---|---|---|---|---|
| Velocity 0.01 m/s | - | - | - | - |
| Scenario 1 | 4,27 | 7,93 | 3,96 | 20,47 |
| Scenario 2 | 4,27 | 7,91 | 3,93 | 20,47 |
| Scenario 3 | 4,26 | 7,90 | 3,91 | 20,48 |
| Velocity 0.375 m/s | - | - | - | - |
| Scenario 1 | 44,60 | 82,30 | 39,24 | 57,71 |
| Scenario 2 | 44,43 | 81,99 | 40,09 | 57,80 |
| Scenario 3 | 44,62 | 82,32 | 39,29 | 57,75 |
| Velocity 0.75 m/s | - | - | - | - |
| Scenario 1 | 94,48 | 174,40 | 75,47 | 91,91 |
| Scenario 2 | 94,26 | 174,00 | 75,16 | 91,80 |
| Scenario 3 | 94,52 | 174,48 | 75,60 | 91,57 |
| Velocity 1.0 m/s | - | - | - | - |
| Scenario 1 | 94,51 | 174,45 | 75,26 | 92,24 |
| Scenario 2 | 96,32 | 177,80 | 76,46 | 94,22 |
| Scenario 3 | 96,44 | 178,02 | 76,51 | 94,33 |
| Velocity 1.25 m/s | - | - | - | - |
| Scenario 1 | 96,32 | 177,80 | 76,44 | 94,18 |
| Scenario 2 | 96,32 | 177,80 | 76,48 | 94,14 |
| Scenario 3 | 96,32 | 177,80 | 76,50 | 94,02 |
| Velocity 3.0 m/s | - | - | - | - |
| Scenario 1 | 96,32 | 177,80 | 76,44 | 94,17 |
| Scenario 2 | 96,32 | 177,80 | 76,54 | 94,10 |
| Scenario 3 | 97,09 | 178,91 | 76,35 | 95,31 |
| Velocity 6.0 m/s | - | - | - | - |
| Scenario 1 | 96,32 | 177,81 | 76,49 | 94,17 |
| Scenario 2 | 96,32 | 177,80 | 76,54 | 94,10 |
| Scenario 3 | 97,09 | 178,91 | 76,28 | 95,31 |

Table 8. The stresses encountered at each velocity within each scenario

| | Equivalent stress avg (mpa) 0,01 m/s | Equivalent stress avg (mpa) 0,75 m/s | Max Shear stress avg (mpa) 0,01 m/s | Max Shear stress avg (mpa) 0,75 m/s | Min Principal stress (mpa) 0,01 m/s | Min Principal stress (mpa) 0,75 m/s | Max Principal stress (mpa) 0,01 m/s | Max Principal stress (mpa) 0,75 m/s |
|---|---|---|---|---|---|---|---|---|
| Scenario 1 Sandstone | 7,93 | 174,40 | 4,27 | 94,48 | 3,96 | 75,47 | 20,47 | 91,91 |
| Scenario 1 Limestone | 7,85 | 159,22 | 4,23 | 86,24 | 6,75 | 106,31 | 22,50 | 142,33 |
| Scenario 1 Dolomite | 7,58 | 151,14 | 4,08 | 81,89 | 6,30 | 139,83 | 24,92 | 176,90 |
| Scenario 2 Sandstone | 7,91 | 174,00 | 4,27 | 94,26 | 3,93 | 75,16 | 20,47 | 91,80 |
| Scenario 2 Limestone | 7,83 | 158,84 | 4,22 | 86,04 | 6,72 | 106,03 | 22,50 | 142,16 |
| Scenario 2 Dolomite | 7,56 | 150,78 | 4,07 | 81,69 | 6,26 | 139,11 | 24,92 | 177,00 |
| Scenario 3 Sandstone | 7,90 | 174,48 | 4,26 | 94,52 | 3,91 | 75,60 | 20,48 | 91,57 |
| Scenario 3 Limestone | 7,82 | 159,31 | 4,21 | 86,30 | 6,70 | 105,81 | 22,50 | 142,55 |
| Scenario 3 Dolomite | 7,55 | 151,21 | 4,06 | 81,93 | 6,24 | 139,36 | 24,92 | 176,80 |

Table 9. Stress changes for each different rock type

| | Deformation avg mm | Deformation avg mm | Volumetric change cm3 | Volumetric change cm3 |
|---|---|---|---|---|
| Velocity | 0,01 m/s | 0,75 m/s | 0,01 m/s | 0,75 m/s |
| Scenario 1 Sandstone | 0,02 | 0,24 | 0,00 | 0,87 |
| Scenario 1 Limestone | 0,14 | 0,23 | 0,00 | 0,84 |
| Scenario 1 Dolomite | 0,13 | 0,21 | 0,00 | 0,79 |
| Scenario 2 Sandstone | 0,02 | 0,24 | 0,00 | 0,87 |
| Scenario 2 Limestone | 0,14 | 0,25 | 0,00 | 0,84 |
| Scenario 2 Dolomite | 0,13 | 0,23 | 0,00 | 0,80 |
| Scenario 3 Sandstone | 0,02 | 0,40 | 0,00 | 0,87 |
| Scenario 3 Limestone | 0,14 | 0,35 | 0,00 | 0,84 |
| Scenario 3 Dolomite | 0,13 | 0,33 | 0,00 | 0,79 |

Table 10. Deformation and volumetric change for each cement scenario and rock type

| Hole Depth (m) | Minimum Horizontal stress (mpa) | Maximum horizontal stress (mpa) | Sandstone Fracture pressure (mpa) | Circumferential stress (mpa) | Radial stress (mpa) |
|---|---|---|---|---|---|
| 6248 | 79,15 | 84,00 | 119,07 | 110,10 | 57,36 |
| 6249 | 79,16 | 84,01 | 119,09 | 110,11 | 57,37 |
| 6250 | 79,18 | 84,03 | 119,11 | 110,13 | 57,38 |
| 6251 | 79,19 | 84,04 | 119,12 | 110,15 | 57,39 |
| 6252 | 79,20 | 84,05 | 119,14 | 110,17 | 57,40 |
| 6253 | 79,21 | 84,07 | 119,16 | 110,18 | 57,41 |
| 6254 | 79,23 | 84,08 | 119,18 | 110,20 | 57,42 |
| 6255 | 79,24 | 84,09 | 119,20 | 110,22 | 57,43 |
| 6256 | 79,25 | 84,11 | 119,22 | 110,24 | 57,44 |
| 6257 | 79,26 | 84,12 | 119,24 | 110,25 | 57,45 |
| 6258 | 79,28 | 84,13 | 119,26 | 110,27 | 57,46 |
| 6259 | 79,29 | 84,15 | 119,28 | 110,29 | 57,47 |
| 6260 | 79,30 | 84,16 | 119,30 | 110,30 | 57,47 |

Table 11. Hand calculation results for Radial and Circumferential stress (mpa)

# A.2 Background to the simulation methodology

Hooke's law, stress linked directly with strain. Calculate deflections and deformation as a measurement of the response of a structure under stress. The use of the finite volume method as the approach that will be chosen as it is a cell centred approach. This method expects to have a linear variation around the central point in the centroid.

Problem Dimensionality. 2D/3D depending on computing resources. The model will be transient, with both fluids and solids present so there for it is a multiphase model. The fluids and solids will be compressible in a turbulent and laminar flow regime. The fluids will be viscous and will be between plastic and elastic in terms of ductility. There will be heat transfer and a solid/fluid interaction with additional forces present along with fluid motion.

## A.2.1 Conservation laws

The conservation laws are focused on Mass, Momentum (linear and angular) and Energy. They are based on the idea of a rate of change of a particular quantity in a volume, which comes from:

- Net Flow of the quantity through the surface of the volume
- Source of the quantity on the volume surface
- Source of the quantity in the volume.

### A.2.1.1 Conservation of Mass

This is also called the continuity equation.

$$\frac{\partial \rho}{\partial t} + \nabla. (\rho u) = 0 \tag{10}$$

Where,
- $\nabla \cdot$ is divergence,
- $\rho$ is fluid density,
- $t$ is time,
- $u$ is the flow velocity vector field.

The idea behind having a control volume is to consider applied physics laws on an infinitesimally small volume and extrapolate this behaviour on an arbitrary volume afterwards. Using the control volume will inherently conserve the flux of the considered quantity, thus leading to the conservative form of the equations. This form can always be manipulated into a non-conservative form. The conservative form has an advantage as it allows for discontinuous solutions.

The material control volume is a mathematical abstraction of a fixed space through which the continuum flows. Its boundary, forms a surface called the control surface.

The integral form or differential forma of the continuity equation utilises the Gauss theorem in order to transform the divergence term acting on the volume to a surface integral.

## A.2.1.2 Conservation of Linear and Angular Momentum

The conservation of linear momentum is the same as Newton's second law of motion, where (F) is force and (p) is momentum. The angular momentum relates to torque (N/m) Forces acting on the control volume are split between the body forces (Fb) and the surface forces transformed into the Cauchy stress tensor (T). The body forces are in the form of the force density, that is for per unit volume. Body forces are typically gravity, electromagnetic forces, centrifugal and Coriolis forces.

The stresses can be interpreted as contact forces on the control volume boundary. Surface forces are for example stresses and static pressures.

$$\frac{\partial \rho u}{\partial t} + \nabla.(\rho u u) = \nabla.T + f_b \tag{11}$$

$$\frac{\partial \rho(r \times u)}{\partial t} + \nabla.\big(\rho u(r \times u)\big) = (r \times \nabla.T) + (r \times f_b) \tag{12}$$

Where,
- T is the Cauchy stress tensor
- Fb are the body forces
- u is velocity

(Rate of increase in momentum in the parcel) = (Sum of forces acting on the parcel). The conservation of angular momentum requires that the Cauchy stress tensor (T) has to be symmetrical in order to satisfy the conservation of linear momentum.

## A.2.1.3 Conservation of Energy

The first law of thermodynamics expressed using the specific total energy (e), where (E) is the total energy and (m) is the mass.

$$\frac{\partial \rho e}{\partial t} + \nabla.(\rho u e) = \nabla.q + \rho Q + \nabla.(T \times u) + f_b \times u \tag{13}$$

Where,
- e is total energy
- T is temperature
- $\rho$ is pressure
- q is the heat flux
- Q is the volumetric energy source
- F is force
- u is velocity

Rate of increase in energy of the parcel = Net rate of heat added to the parcel + Net rate of work done on the parcel.

Physical properties of the system can be classified as intensive or extensive quantities. Intensive properties are independent of the system size and the material amount, for example temperature (T) or pressure ($\rho$). Extensive properties are connected to the system size dependency, which is cumbersome if we consider parcels of matter, specific properties are defined by normalization of extensive properties by mass.

The net rate of heat added to the parcel is based on the heat flux (q) through the parcel's surface and the volumetric energy sources (Q)

The net rate of work done on the parcel is the product of the force (F) and velocity (u).

## A.2.2 Discretization Methods

After the mathematical model has been selected the correct discretization method has to be chosen. This is to have a method to approximate the differential equations to be used by using a system of algebraic equations for the variables at a set of discrete locations in space and time. (Ferziger and Peric 2002) There are a few different approaches, but the most important are the finite difference, finite volume and finite element methods.

### A.2.2.1 Finite Difference Method

This is the oldest method for numerical solution of partial differential equations (PDE's), believed to have been introduced by Euler in the 18th century. It is also the easiest method to use for simple geometries. (Ferziger and Peric 2002)

The starting point is the conservation equation in a differential form. The solution domain is covered by a grid. At each grid point, the differential equation is approximated by replacing the partial derivatives by approximations in terms of the nodal values of the functions. This results in having one algebraic equation per grid node or point, so that the variable value at that and a certain number of neighbour nodes appear as unknowns. (Ferziger and Peric 2002)

In principle, the finite difference method can be applied to any grid type but according to Ferziger and Peric in 2002 this method has only been applied to structured grids. The grid lines that make up this structured grid work as local coordinate lines.

The Taylor series expansion or polynomial fitting is used to then obtain approximations to the first and second derivatives of the variables with respect to the given coordinates. When needed these methods are used to obtain variable values at locations other than grid nodes by using a process of interpolation. (Ferziger and Peric 2002)

On structured grids, the finite difference method is very simple and effective. It is especially easy to obtain higher-order schemes on regular grids. The disadvantage of finite difference method is that the conservation laws are not enforced unless particular care is taken. Also, there is a restriction to simple geometries which is a significant disadvantage in complex flows. (Ferziger and Peric 2002)

### A.2.2.2 Finite Volume Method

The finite volume method uses the integral form of the conservation equations as its starting point. (Ferziger and Peric 2002) The solution domain is subdivided into a finite number of contiguous control volumes and the conservation equations are applied to each control volume.

At the centroid of each control volume lies a computational node at which the variable values are to be calculated. Interpolation is used to express variable values at the control volume's surface. (Ferziger and Peric 2002)

The finite volume method can accommodate any style of grid, so it is suitable for both simple and complex geometries. The grid only sets out the control volume boundaries and don't need to be related to a coordinate system.

The finite volume approach is perhaps the simplest to understand and to program. (Ferziger and Peric 2002)

The disadvantage of finite volume methods compared to finite difference schemes is that methods with an order higher than two are more difficult to develop in three dimensions. This is due to the fact that the finite volume approach requires three levels of approximation: interpolation, differentiation, and integration. (Ferziger and Peric 2002)

## A.2.2.3 Finite Element Method

The finite element method is similar to the finite volume method in many ways. The domain is broken into a set of discrete volumes or finite elements that are generally unstructured; in 2D, they are usually triangles or quadrilateral shapes, while in 3D tetrahedral or hexahedral shapes are most often used. (Ferziger and Peric 2002)

The distinguishing feature of finite element methods is that the equations are multiplied by a 'weight function' before they are integrated over the entire area. In the least complicated finite element methods, the solution is approximated by a shape function that is linear within each of the elements in a way that guarantees continuity of the solution across all the element boundaries. This kind of function can be constructed from values at the corners of the elements. (Ferziger and Peric 2002)

This approximated solution is then applied to the weighted integral of the conservation law and the equations that are solved are derived by requiring the derivative of the integral with respect to each nodal value to be zero; this corresponds to selecting the best solution within the set of allowed functions which is basically the one with the smallest residual error. This results in a set of non-linear algebraic equations. (Ferziger and Peric 2002)

An important advantage of the finite element method is the ability to deal with random geometries. The grids are easily refined, each element is simply split. Finite element methods are relatively easy to analyse mathematically and can be shown to have optimality properties for certain types of equations. The principal drawback, which is shared by any method that uses unstructured grids, is that the matrices of the linearized equations are not as well organised as those for regular grids making it more difficult to find an efficient solution method. (Ferziger and Peric 2002)

A hybrid method called control-volume-based finite element method should also be mentioned. In this method shape functions are used to describe variations in the variables around a particular element. Control volumes are formed around each node by joining the centroids of the elements. The conservation equations in integral form are applied to the control volumes in the same way as with the finite volume method. The fluxes through the control volume boundaries and the source terms are calculated. (Ferziger and Peric 2002)

## A.2.3 Constitutive relations

Constitutive relations establish a certain functional dependence between physical quantities and are usually specific to the material or substance. They provide a mathematical closure to help solve conservation equations. They are commonly required to satisfy the second law of thermodynamics that says that the thermodynamic process id irreversible by stating that the specific entropy of the system always increases. Entropy is defined as a thermodynamic property which serves as a measure of how close a system is to equilibrium.

### A.2.3.1 Internal Energy and Enthalpy

Energy conservation law uses the term total energy which is also known as the sum of all the energy forms. Enthalpy represents the total heat content of the thermodynamic system. In this system the physical properties can be classified as either intensive of extensive quantities.

Intensive properties are independent of the system size or the material amount such as temperature or pressure.

The Extensive properties are connected to the system size and are added to the system, mass is an example. To detach the system from this size dependency which can be bulky if we consider parcels of matter, precise properties are defined by the normalization of extensive properties by mass.

The specific internal energy is a function of pressure and temperature. Then there is specific kinetic energy which is connected to the motion and then also there is enthalpy which describes the energy changes in the system if there is a connection to a constant pressure.

### A.2.3.2 Fourier's Law

Fourier's Law or the Law of heat conduction, states that the time rate of heat transfer through a material is proportional to the negative gradient in the temperature and to the area at right angles to that gradient, through which the heat is flowing or in simple terms, that heat moves from hot to cold. Warm molecules within the material vibrate and transfer their vibrations onto colder molecules that vibrate less.

This law can be stated in two equivalent forms. One being the integral form, in which one considers the amount of energy flowing into or out of a body as a whole and the second being the differential form, in which one considers the local flows or fluxes of energy. (Baierlein 1999)

### A.2.3.3 Equation of state and transport coefficients

The equation of state links together properties of the system that depend on the current thermodynamic state, this is expressed as:

$$\rho = \rho(p, T) \tag{14}$$

Where,
- $\rho$ is density
- $p$ is pressure
- $T$ is temperature

Transport coefficients are also linked to the thermodynamic state of the system such as the viscosity and the heat conduction coefficient.

## A.2.3.4 Hooke's Law

The strain of an elastic material is proportional to the stress applied to it. Hooke observed behaviour of springs. or relatively small deformations of an object, the displacement or size of the deformation is directly proportional to the deforming force or load. Under these conditions the object returns to its original shape and size upon removal of the load. Elastic behaviour of solids according to Hooke's law can be explained by the fact that small displacements of their constituent molecules, atoms, or ions from normal positions is also proportional to the force that causes the displacement. (The Editors of Encyclopaedia Britannica 2017)

$$F = -k\,s \tag{15}$$

Where,
- F is force (N)
- k is spring constant (N/m)
- s is extension or compression distance (m)

## A.2.3.5 Stress in a fluid

Stresses express the internal forces in the fluid. A fluid is unable to sustain shear stress at rest, therefore shear stresses are connected to fluid motion.
Stress in two parts:

1. Hydrostatic stress – fluid volumetric changes capturing hydrostatic pressure.
2. Shear stress – shape distortions, rate of strain relationship between shear stresses and shear rate, this is also known as dynamic viscosity.

The strain rate is material deformation over a time period that contains both the expansion rate, volumetric change and shear rate that is progressive shearing without a volumetric change.

## A.2.3.6 Types of fluid

There are 3 main types of fluids that are modelled.

1. Inviscid fluid, this is an ideal fluid model governed by Euler equations
2. Newtonian fluids

   This is a fluid that has a linear relationship between viscosity and shear stress. The viscosity remains constant no matter the amount of shear applied at a constant temperature.
3. Non-Newtonian fluids are materials that do not follow the Newtonian linear dependency between strain rates and shear stresses.
   The 3 types of Non-Newtonian fluid are;
   a. Power Law
   b. Herschel-Buckley

c. Bingham Plastic

Their relationship to each other and stress and strain can be seen in the diagram below. The Herschel Buckley model is what the cement slurry is based on as this best represents cement slurry behaviour, as it is a non-Newtonian visco-plastic fluid. It is described by a non-linear constitutive law containing three rheological parameters determined experimentally, these include consistency,
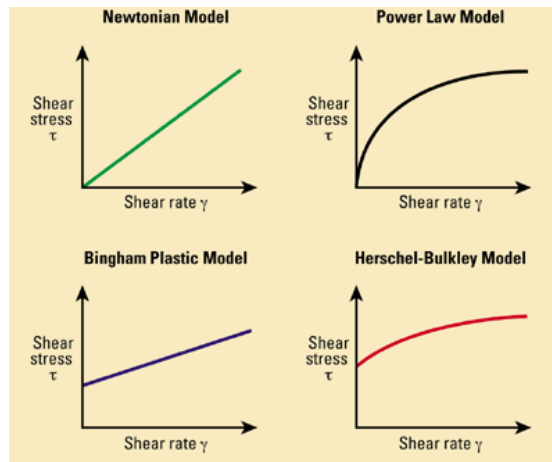
Figure 35. Newtonian and Non-Newtonian fluid rheological models (drillingformulas.com 2010)

the power law index and the yield stress. (Taibi and Messelmi 2017)

The equation used for the Herschel Bulkley fluid in turbulent flow is the following:

$$Pl = \frac{7.48 * f * (0.002217 * Q)^2 * p}{0.005712 * (D_2 - D_1) * (D_2^2 - D_1^2)^2} \tag{16}$$

(Elmgerbi, et al. 2016)

Where,

- f is Friction Factor [Dimensionless]
- Q is Flow rate [gpm, m3/second]
- p is pressure
- $D_2$ is open hole diameter [in, m]
- $D_1$ is Casing outer diameter [in, m]

## A.2.3.7 Couette flow

In Figure 36, the difference between the flow of an incompressible fluid between two plates. A has now pressure gradient with the top plate moving and b has a pressure gradient but both plates are stationary and show fully developed flow.
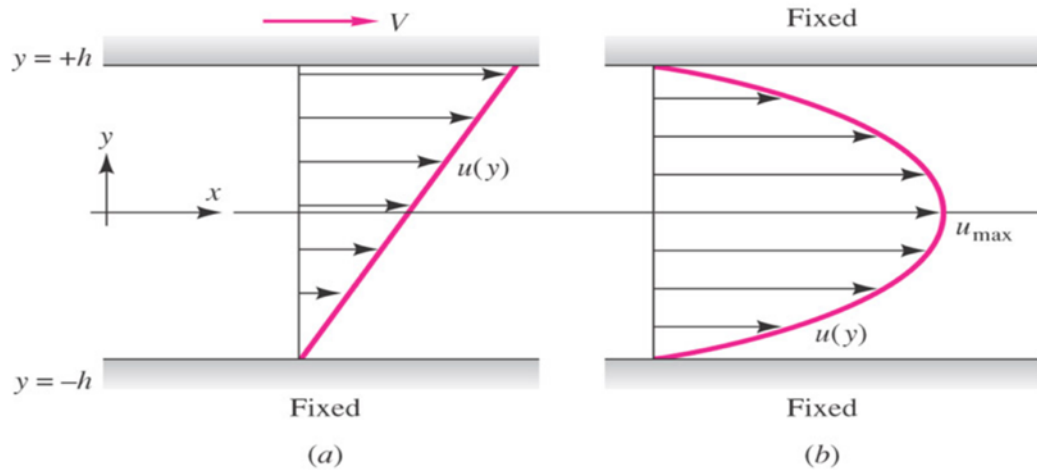
Figure 36. Incompressible viscous flow between parallel plates, a) no pressure gradient; b) pressure gradient with both plates fixed.   (Bahrami 2009)

## A.2.3.8 Navier Stokes equations

The Navier-Stokes equations for compressible flow describe a fluid where the density is linked to the thermodynamic state of the system. So, the density is considered to be a function of both pressure and temperature with no simplification involved. As a consequence, the energy equation is an integral part of the problem and has to be solved together with momentum and continuity. (Łukaszewicz and Kalita 2016) Ansys uses this system of equations in fluent. An example of these equations can be seen below:

$$1: \frac{\partial \rho}{\partial t} + \nabla.(\rho u) = 0 \tag{17}$$

$$2: \frac{D}{Dt}(\rho u) = -\nabla \left(p + \frac{2}{3}\mu \nabla.u\right) + \nabla.(\mu[\nabla u + (\nabla u)^T]) \tag{18}$$

$$3: \frac{\vartheta}{\vartheta t}(\rho h) + \nabla.(\rho u h) = \frac{\vartheta p}{\vartheta t} + \nabla.(up) - p\nabla.u + \nabla.(\alpha \nabla h) \tag{19}$$

$$4: \rho = \rho(p, T) \tag{20}$$

$$5: \mu = \mu(p, T), \alpha = \alpha(p, T) \ etc \dots \tag{21}$$

(Łukaszewicz and Kalita 2016)

## A.2.3.10 Face Flux

The face of mass flux is a scalar that describes both the mass inflow and outflow through the face of the control volume. Geometrically, the face flux can be interpreted as a projection of $(\rho u_f)$ on the face areas vector S.
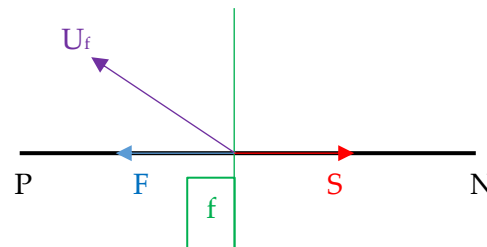


$$F = S \cdot (\rho u_f) \tag{22}$$

Where,
- F is Face flux
- S is the face area vector
- $\rho u_f$ is pressure, velocity flux

# Bibliography

Łukaszewicz, Grzegorz, und Piotr Kalita. 2016. *Navier–Stokes Equations An Introduction with Applications.* Switzerland: Springer International Publishing .

Al-Tahini, Ashraf M, und Younane N Abousleiman. 2008. „Insights into borehole deformation and relationship between wellbore induced stresses, breakouts, and in-situ stresses." *the 42nd US Rock Mechanics Symposium and 2nd U.S.-Canada Rock Mechanics Symposium.* San Francisco: American Rock Mechanics Association .

Bahrami, M. 2009. *Differential Relations for Fluid Flow.* Zugriff am 10. February 2019. http://www.sfu.ca/~mbahrami/ENSC%20283/Notes/Differential%20Relations%20for%20Fluid%20Flow.pdf.

Baierlein, Ralph. 1999. *Thermal Physics.* Cambridge: University Press, Cambridge.

Clement, William P. 2008. *Writting and Thinking Well.* 2 February. Accessed July 13, 2016. http://cgiss.boisestate.edu/~billc/Writing/writing.html.

Cook, John, René A Frederiksen, Klaus Hasbo, Sidney Green, Arnis Judzis, J. Wesley Martin, Roberto Suarez-Rivera, et al. 2007. „Rocks Matter: Ground Truth in Geomechanics." *Oilfield Review*, 1. October: 36-55. https://www.slb.com/~/media/Files/resources/oilfield_review/ors07/aut07/rocks_matter.pdf.

Drilling and Completion Committee. 2017. „Primary Cementing An Industry Recommended Practice (IRP) for the Canadian Oil and Gas Industry." *Drilling and completion Committee* (Enform) 25 (1): 1-165.

drillingformulas.com. 2010. *drilling formulas.* Zugriff am 28. March 2018. http://www.drillingformulas.com/drilling-fluid-properties/.

Earle , S. 2015. *Physical Geology.* 1st Edition. BC Campus: Pressbooks. Zugriff am 30. December 2018. https://opentextbc.ca/geology/chapter/12-1-stress-and-strain/.

Economides, Michael J. 1992. *A Practical Companion to Reservoir Stimulation.* London: Elsevier.

Elmgerbi, Asad , Gerhard Thonhauser, Michael Prohaska, Abbas Roohi , und Andreas Nascimen. 2016. „General Analytical Solution for Estimating the Elastic Deformation of an Open Borehole Wall." *International Journal of Scientific & Engineering Research* 1056-1068.

Elmgerbi, Asad, Gerhard Thonhauser, Michael Prohaska, Abbas Roohi, und Andreas Nascimento. 2016. „Application of Computer Programming to Estimate Volumetric Change of an Active Drilling Fluid System Cause by Elastic Deformation of an Open Borehole Section Wall." *Global Journal of Computer Science and Technology: Information & Technology* 16 (3): 15-29.

Ferziger, J H, und M Peric. 2002. *Computational Methods for Fluid dynamics.* 3rd Edition. Berlin: Springer-Verlag.

Fjær, Erling , Rune M. Holt, Per Horsrud, und Arne M. Ra. 1992. „Chapter 4 Stresses around boreholes, and borehole failure criteria." *Developments in Petroleum Science* (Elsevier) Volume 33: 109-134.

Fluent Inc. 2006. *FLUENT User's Guide.* 20. 09. Zugriff am 20. 02 2019. https://www.sharcnet.ca/Software/Fluent6/html/ug/main_pre.htm.

George E King Consulting. 2011. *http://gekengineering.com/id6.html.* Zugriff am 19. 02 2018. http://gekengineering.com/Downloads/Free_Downloads/Cementing_Chapter_3 .pdf.

Hagura, Junichi. 2003. „Cementing Deepwater Wells." 24. june. Zugriff am 6. December 2018. https://www.japt.org/html/iinkai/drilling/bunkakai/daisuisinn/data/PresenJour nal/H15Symposium_Deepwater_Cementing_Presen.pdf.

Helstrup, A, M K Rahman , M M Hossain, und S Rahman. 2001. „A Practical Method for Evaluating Effects of Fracture Charging and/or Ballooning When Drilling High Pressure, High Temperature (HPHT) Wells." *SPE/IADC Drilling Conference.* Amsterdam: SPE.

Lavrov, A, und J Tronvoll. 2005. „Mechanics of Borehole Ballooning in Naturally-Fractured Formations." Bahrain: Society of Petroleum Engineers.

Norwegian University of Science and Technology. 2012. *An Introduction to Well Integrity.* Trondheim.

Ozdemirtas, M, T Babadagli, und E Kuru. 2007. „Numerical Modelling of Borehole Ballooning/Breathing - Effect of Fracture Roughness." *Canadian International Petroleum Conference.* Calgary: PETROLEUM SOCIETY CANADIAN INSTITUTE OF MINING, METALLURGY & PETROLEUM.

Schlumberger. 2018. *Oilfield Glossary: elastic deformation.* https://www.glossary.oilfield.slb.com/Terms/e/elastic_deformation.aspx.

—. 2018. *Oilfield Glossary: plastic deformation.* https://www.glossary.oilfield.slb.com/Terms/p/plastic_deformation.aspx.

Taibi, H, und F Messelmi. 2017. „Effect of yield stress on the behaviour of rigid zones during the laminar flow of Herschel-Buckley fluid." *Science Direct.* Alexandria Engineering Journal . 2. February. Zugriff am 08. October 2018. https://www.sciencedirect.com/science/article/pii/S1110016817300030.

The Editors of Encyclopaedia Britannica. 2017. *Encyclopaedia Britannica Hookes law.* 15. December. Zugriff am 10. February 2019. https://www.britannica.com/science/Hookes-law.

Therond, E, S Taoutaou, S G James, P W Way, P Gomes, und A Dondale. 2018. „Understanding Lost Circulation While Cementing: Field Study and Laboratory Research." *SPE Drilling & Completion* (SPE 184673): 77-86.

# Acronyms

| | |
|---|---|
| *FE* | Finite Element |
| *Q* | Density (kg/m3) |
| υ | Mean velocity (m/sec) |
| $Y_p$ | Yield point [Ib/100ft.] |
| σh | Minimum horizontal principle stress [Psi, Pa] |
| $\sigma\sigma_{HH}$ | Maximum horizontal principle stress [Psi, Pa] |
| $\sigma\sigma_{vv}$ | Vertical principle stress [Psi, Pa] |
| $P_P$ | Formation pore pressure [Psi, Pa] |
| $\upsilon\upsilon$ | Poisson ratio [Dimensionless] |
| $\alpha$ | Biot's elastic constant [Dimensionless] |
| $P_w$ | Borehole Pressure [Psi, Pa] |
| u | Radial elastic displacement for the borehole [in, m] |
| r | Wellbore radius [in, m] |
| E | Young's modulus [Psi, Pa] |
| η | Poroelastic stress coefficient [Dimensionless] |
| n | Behaviour Index [Dimensionless] |
| k | Consistency Index [EqcP] |
| f | Friction Factor [Dimensionless] |
| $C_a$ | Herschel Bulkley variable [Dimensionless] |
| Q | Flow rate [gpm, m3/second] |
| $PP_{ff}$ | Fracture initiation pressure [Psi, Pa] |
| ɸ | Rock frication angle [$^0$] |
| $^{\Delta t}$ | Thermal stress [Psi, Pa] |
| T | Rock tensile strength [Psi, Pa] |
| p*w* | Collapse pressure [Psi, Pa] |
| S₀ | Rock cohesive strength [Psi, Pa] |

# Symbols

| | | |
|---|---|---|
| $m$ | mass | [kg] |
| $r$ | radius | [m] |

# List of Figures

# List of Tables